Musical expertise shapes functional and structural brain networks independent of absolute pitch ability

Short Title

Functional and structural connectivity in musicians

Authors

Simon Leipold [a, b, $], Carina Klein [a, $], Lutz Jäncke [a, c, d]

[$] These authors contributed equally to this work

Author Affiliations

[a] Division Neuropsychology, Department of Psychology, University of Zurich, Zurich, Switzerland

[b] Department of Psychiatry and Behavioral Sciences, Stanford University School of Medicine, Stanford, USA

[c] University Research Priority Program (URPP), Dynamics of Healthy Aging, University of Zurich, Zurich, Switzerland

[d] Department of Special Education, King Abdulaziz University, Jeddah, Kingdom of Saudi Arabia

Corresponding Authors

Simon Leipold
1070 Arastradero Rd.
Palo Alto, CA 94304
United States of America
leipold@stanford.edu

Lutz Jäncke
Binzmühlestrasse 14, Box 25
CH-8050 Zürich
Switzerland
lutz.jaencke@uzh.ch

Abstract

Professional musicians are a popular model for investigating experience-dependent plasticity in human large-scale brain networks. A minority of musicians possess absolute pitch, the ability to name a tone without reference. The study of absolute pitch musicians provides insights into how a very specific talent is reflected in brain networks.

Previous studies of the effects of musicianship and absolute pitch on large-scale brain networks have yielded highly heterogeneous findings regarding the localization and direction of the effects. This heterogeneity was likely influenced by small samples and vastly different methodological approaches.

Here, we conducted a comprehensive multimodal assessment of effects of musicianship and absolute pitch on intrinsic functional and structural connectivity using a variety of commonly employed and state-of-the-art multivariate methods in the largest sample to date (n = 153; 52 absolute pitch musicians, 51 relative pitch musicians, and 50 non-musicians).

Our results show robust effects of musicianship in inter- and intrahemispheric connectivity in both structural and functional networks. Crucially, most of the effects were replicable in both musicians with and without absolute pitch when compared to non-musicians. However, we did not find evidence for an effect of absolute pitch on intrinsic functional or structural connectivity in our data: The two musician groups showed strikingly similar networks across all analyses.

Our results suggest that long-term musical training is associated with robust changes in large-scale brain networks. The effects of absolute pitch on neural networks might be extremely subtle, requiring very large samples or task-based experiments to be detected.

Introduction

Professional musicians are a commonly studied model for experience-dependent brain plasticity (Herholz and Zatorre, 2012; Jäncke, 2009; Münte et al., 2002; Schlaug, 2015). Intense musical training starting early in life is thought to cause neuroplastic adaptations that are paralleled by improvements in audition, sensory-motor skills, and possibly higher-order cognitive functions (Fujioka et al., 2006; Habibi et al., 2018; Hyde et al., 2009; Schlaug et al., 2009; Seither-Preisler et al., 2014). In recent years, a major focus within the neuroscience of music has been on training-related plasticity in large-scale brain networks, which underlie most human sensory, motor, and cognitive functions (Bressler and Menon, 2010; Mesulam, 1990; Sporns et al., 2004).

Using various imaging methods, some evidence has been accumulated that musicianship is associated with differences in both the intrinsic functional and structural networks of the human brain. However, a detailed examination of these studies reveals inconsistencies in findings regarding the location of the effects in the brain and also the direction of these effects. For example, while most of the studies report hyperconnectivity in musicians compared to non-musicians (Fauvel et al., 2014; Klein et al., 2016; Palomar-García et al., 2017; Zamorano et al., 2017), others have found hypoconnectivity (Imfeld et al., 2009), or even effects in both directions depending on the brain regions or tracts (Acer et al., 2018; Bengtsson et al., 2005; Luo et al., 2014; Schmithorst and Wilke, 2002). These studies show that in musicians, connectivity between brain regions is altered across the entire brain including not only sensory, motor, multisensory, and cognitive regions of the cortex (Belden et al., 2020; Fauvel et al., 2014; Klein et al., 2016; Palomar-García et al., 2017), but also subcortical brain regions (Gujing et al., 2019; Luo et al., 2014, 2012; Schmithorst and Wilke, 2002; Zamorano et al., 2019, 2017), and even the cerebellum (Abdul-Kareem et al., 2011; Belden et al., 2020; Luo et al., 2014, 2012; Schmithorst and Wilke, 2002).

The diversity of these findings could be influenced by small sample sizes and inconsistent methodology. In studies examining intrinsic functional connectivity, the number of participants in the musician groups ranged from 11 (Zamorano et al., 2017) to 25 (Luo et al., 2014), and in studies examining structural connectivity, from only five (Schmithorst and Wilke, 2002) to 36 (Steele et al., 2013). Studies with small samples lack the statistical power to detect small effects, and findings from small-scale studies have a higher probability of returning false positives (Button et al., 2013). With regard to methodology, many previous studies took a region of interest (ROI)-based approach. Concerning functional networks, the seeds of different studies have essentially covered the entire cortex (Belden et al., 2020; Fauvel et al., 2014; Gujing et al., 2019; Luo et al., 2012; Palomar-García et al., 2017; Zamorano et al., 2019, 2017). To our knowledge, only two functional connectivity studies exist using a data-driven, connectomic whole-brain approach (Klein et al., 2016; Luo et al., 2014). In one of these, Klein et al. (2016) showed effects of musicianship on electrophysiological networks in brain regions closely related to the perception and production of music. Studies on structural networks in musicians have exclusively used an ROI-based approach by focusing on

separate white-matter tracts or brain regions (Abdul-Kareem et al., 2011; Bengtsson et al., 2005; Bouhali et al., 2020; Elmer et al., 2016; Halwani et al., 2011; Imfeld et al., 2009; Oechslin et al., 2010a; Rüber et al., 2015; Schlaug et al., 1995; Schmithorst and Wilke, 2002; Steele et al., 2013; Vollmann et al., 2014). No previous structural connectivity study comparing musicians and non-musicians has employed a whole-brain connectomic approach.

Apart from general effects of musicianship on large-scale brain networks, some studies have focused on a special talent present among musicians: absolute pitch (AP), the rare ability to name a tone without reference (Deutsch, 2013). Musicians without AP use relative pitch (RP) to identify tones by harnessing the relationships between different tones. Only a few studies examined intrinsic functional networks in AP versus RP musicians. Again, the findings of these studies show little consistency, suggesting an effect of AP on functional connectivity of primary and secondary sensory, parietal, and frontal brain regions (Brauchli et al., 2019; Elmer et al., 2015; Kim and Knösche, 2017). The applied methodology differed widely between studies, with some studies using an ROI-based approach (Brauchli et al., 2019; Elmer et al., 2015; Kim and Knösche, 2017), and other studies using an whole-brain approach (Jäncke et al., 2012; Loui et al., 2012; Wenhart et al., 2019). An effect of AP on structural connectivity (using diffusion parameters) has been reported for various subregions in the vicinity of associative auditory areas (Burkhard et al., 2020; Dohn et al., 2015; Kim and Knösche, 2016; Loui et al., 2011). One study found an enhanced asymmetry in diffusion parameters in the superior longitudinal fasciculus (Oechslin et al., 2010a). None of the previous studies investigating AP and structural connectivity employed a whole-brain connectomic approach. Importantly, all of these results have yet to be replicated in an independent sample.

Taken together, findings from previous studies regarding the effects of musicianship and AP on functional and structural networks are highly inconsistent, possibly due to small samples and methodological differences. In this study, we aimed to identify robust effects of musicianship and AP on functional and structural connectivity using a multitude of previously employed and novel methods on a large multimodal dataset (n = 153), consisting of 52 AP musicians, 51 RP musicians, and 50 non-musicians. In particular, we employed both ROI-based and whole-brain approaches as well as a state-of-the-art multivariate approach based on machine learning algorithms, sensitive for simultaneous hyper- and hypoconnectivity in networks (Haynes, 2015; Uddin et al., 2013). Crucially, we determined if the effects of musicianship were replicable in both musician groups, irrespective of their AP ability.

Materials and methods

Participants

We analyzed resting-state functional magnetic resonance imaging (rsfMRI) and diffusion-weighted imaging (DWI) data of 153 participants. A portion of the rsfMRI data (Brauchli et al., 2019) and the DWI data (Burkhard et al., 2020) was previously analyzed using a different methodology. The participants consisted of three groups: AP musicians (n = 52), RP musicians (n = 51), and non-musicians (n = 50). The groups were comparable regarding sex, handedness, age, rsfMRI movement, and DWI movement (see Table 1). Participants of the musician groups were either professional musicians, music students, or highly trained amateurs. Assignment to the musician groups (AP or RP) was based on self-report and confirmed by a tone-naming test (Oechslin et al., 2010b). During the test, participants had to name 108 pure tones presented in a pseudorandomized order. Octave errors were disregarded in the calculation of the tone-naming score (Leipold et al., 2019a). Non-musicians had not received formal musical training in the five years prior to the study. Demographical (sex, handedness, age) and behavioral data (musical aptitude, musical experience, and tone-naming proficiency) were collected using LimeSurvey (https://www.limesurvey.org/). Self-reported handedness was confirmed using a German translation of the Annett questionnaire (Annett, 1970). Musical aptitude was assessed using the Advanced Measures of Music Audiation (AMMA) (Gordon, 1989). During the AMMA test, participants were presented with short pairs of piano sequences. The participants had to decide whether the sequences were equivalent or differed in tonality or rhythm. None of the participants reported any neurological, audiological, or severe psychiatric disorders, substance abuse, or other contraindications for MRI. All participants provided written informed consent and were paid for their participation or received course credit. The study was approved by the local ethics committee (https://kek.zh.ch/) and conducted according to the principles defined in the Declaration of Helsinki.

Statistical analysis of behavioral data

Participant characteristics were compared between the groups using one-way analyses of variance (ANOVAs) with a between-participant factor *group* or Welch's *t*-tests where appropriate (significance level $\alpha = 0.05$). The analyses were performed in R (version 3.6.0, http://www.r-project.org/). We used the R packages *ez* (version 4.4-0, https://CRAN.R-project.org/package=ez) for frequentist ANOVAs and *BayesFactor* (version 0.9.12-4.2, https://CRAN.R-project.org/package=BayesFactor) for Bayesian ANOVAs (Rouder et al., 2012) and Bayesian *t*-tests (Rouder et al., 2009). We used default priors (scale value r = 0.707) as implemented in the *BayesFactor* package. Consequently, alongside *p* values, we report Bayes factors quantifying the evidence for the alternative relative to the null hypothesis (BF_{10}) and vice versa (BF_{01}) (Kass and Raftery, 1995). Bayes factors are interpreted as evidence for one hypothesis relative to the other hypothesis. A Bayes factor between 1 and 3 is considered as anecdotal evidence, between 3

and 10 as moderate evidence, between 10 and 30 as strong evidence, between 30 and 100 as very strong evidence, and larger than 100 as extreme evidence (Boekel et al., 2015; Jeffreys, 1961). Effect sizes of ANOVA-effects are given as generalized eta-squared (η^2_G) and effect sizes for *t*-tests are given as Cohen's *d*.

MRI data acquisition

Magnetic resonance imaging (MRI) data were acquired using a Philips Ingenia 3.0T MRI system (Philips Medical Systems, Best, The Netherlands) equipped with a commercial 15-channel head coil. For each participant, we acquired whole-brain rsfMRI and DWI data, and a whole-brain anatomical T1-weighted image to facilitate the spatial normalization of the rsfMRI and DWI data. For the musician groups, we also collected fMRI data during a pitch-processing task, which is discussed in another publication (Leipold et al., 2019a). The whole scanning session lasted around 50 minutes.

rsfMRI data acquisition

For the acquisition of rsfMRI data, we used a T2*-weighted gradient echo (GRE) echo-planar imaging (EPI) sequence with the following parameters: repetition time (TR) = 2,300 ms, echo time (TE) = 30 ms, flip angle α = 78°, slice scan order = interleaved, number of axial slices = 40, slice thickness = 3 mm, field of view (FOV) = 220 x 220 x 143 mm^3, acquisition voxel size = 3 x 3 x 3 mm^3; reconstructed to a spatial resolution of 2.75 x 2.75 x 3.00 mm^3 with a reconstruction matrix of 80 x 80, number of dummy scans = 5, total number of scans = 210, total scan duration = 8 min. Participants were instructed to relax and look at a fixation cross during the scanning.

DWI data acquisition

We acquired DWI data using a diffusion-weighted spin echo (SE) EPI sequence with the following parameters: TR = 10,022 ms, TE = 89 ms, acquisition and reconstructed voxel size = 2 x 2 x 2 mm^3, reconstruction matrix = 112 x 112, flip angle α = 90°, FOV = 224 x 224 x 152 mm^3, number of axial slices = 76, B = 1000 s/mm^2, number of diffusion-weighted scans/directions = 64, number of non-diffusion weighted scans = 1, total scan duration = 14 min. Additionally, we acquired six non-diffusion weighted images (B = 0) in opposing phase encoding directions (anterior-posterior, posterior-anterior), which were used during the preprocessing of the DWI data.

T1-weighted MRI data acquisition

The anatomical image was acquired using a T1-weighted GRE turbo field echo sequence with the following parameters: TR = 8.1 ms, TE = 3.7 ms, flip angle α = 8°, number of sagittal slices = 160, FOV = 240 x 240 x 160 mm^3, acquisition voxel size = 1 x 1 x 1 mm^3; reconstructed to a spatial resolution of 0.94 x 0.94 x 1.00 mm^3 with a reconstruction matrix of 256 x 256, total scan duration = 6 min.

MRI data preprocessing

rsfMRI data preprocessing

Preprocessing of the rsfMRI data was performed in MATLAB R2016a (https://ch.mathworks.com/) using DPARSF (version 4.4 _180801, http://rfmri.org/DPARSF/) (Yan and Zang, 2010), which is part of DPABI (version 4.0_190305, http://rfmri.org/dpabi/) (Yan et al., 2016) and uses functions of SPM12 (version 6906, https://www.fil.ion.ucl.ac.uk/spm/). Preprocessing included the following steps: (1) slice time correction using the middle slice as a reference, (2) realignment using a six-parameter (three translations and three rotations) rigid body transformation, (3) coregistration of rsfMRI data and the T1-weighted anatomical image, (4) segmentation of the T1-weighted anatomical image into gray matter, white matter, and cerebrospinal fluid (CSF), and estimation of deformation field for spatial normalization, (5) general linear model-based removal of nuisance covariates including (i) low-frequency trends (first degree polynomial), (ii) effects of head motion estimated by the six realignment parameters and their first temporal derivatives, (iii) five principle components of white matter and cerebrospinal fluid signals using CompCor (Behzadi et al., 2007), and (vi) the global signal (Power et al., 2017), (6) temporal filtering (0.008–0.09 Hz), (7) spatial normalization of rsfMRI data to MNI space using DARTEL (Ashburner, 2007), (8) interpolation to an isotropic voxel size of 3 mm^3, (9) spatial smoothing using an 8 mm full-width-at-half-maximum (FWHM) kernel, and (10) removal of scans ("scrubbing") with framewise displacement (FD) ≥ 0.5 mm, together with the scan immediately before, and together with the two scans immediately after the scan with FD ≥ 0.5 (Power et al., 2012). The quality of spatial normalization was manually inspected.

DWI data preprocessing

Preprocessing of the DWI data was performed in FSL (version 6.0.1, https://fsl.fmrib.ox.ac.uk/fsl/) (Smith et al., 2004). First, we used *topup* to estimate susceptibility-induced and eddy current-induced distortions based on the non-diffusion weighted images acquired in opposing phase encoding directions. Then, we simultaneously corrected for these distortions and for motion artifacts using *eddy* (Andersson and Sotiropoulos, 2016). As a quality control step, we visually checked the orientation of the principal eigenvector (V1) using *DTIFIT* on the preprocessed DWI data.

rsfMRI seed-to-voxel analyses

We examined intra- and interhemispheric functional connectivity between auditory regions of interest (ROIs) and voxels in the temporal, parietal, and frontal lobe. In both hemispheres, the Heschl's gyrus (HG) and the planum temporale (PT) were selected as seed regions. For each participant, we initially computed the functional connectivity between the seed ROIs and all other voxels of the brain using DPABI. The ROIs were based on probability maps of parcels included in the Harvard-Oxford cortical atlas (probability threshold = 25 %). Functional connectivity maps were built by computing the Pearson correlation coefficient between the preprocessed, spatially averaged time-series within an ROI and the preprocessed time-series

of all voxels. To improve the normality of the resulting voxel-wise correlation values, we subsequently applied a Fisher's r-to-z transformation. This resulted in four (one per ROI) z-transformed connectivity maps per participant, which were subjected to second-level analyses.

Group comparisons of functional connectivity maps

To assess the effect of AP, we compared the functional connectivity maps between AP musicians and RP musicians. To assess the effect of musicianship, we compared the functional connectivity maps between RP musicians and non-musicians. To replicate potential effects of musicianship, we additionally compared AP musicians and non-musicians. For all group comparisons we used nonparametric two-sample *t*-tests (threshold-free cluster enhancement [TFCE] inference, 10,000 permutations) in PALM (version alpha115, https://fsl.fmrib.ox.ac.uk/fsl/fslwiki/PALM) (Smith and Nichols, 2009; Winkler et al., 2014). The significance level was set to $\alpha = 0.05$, family-wise error (FWE)-adjusted for multiple comparisons. We restricted the search space of the group comparisons using a mask that included the following bilateral regions of the Harvard-Oxford cortical atlas thresholded at 10 % probability: HG; PT; planum polare (PP); superior temporal gyrus (STG; anterior and posterior division); middle temporal gyrus (MTG; anterior and posterior division); insular cortex; supramarginal gyrus (SMG; anterior and posterior division); angular gyrus; superior parietal lobule; postcentral gyrus (postCG); precentral gyrus (preCG); inferior frontal gyrus, pars opercularis (IFG,po); inferior frontal gyrus, pars triangularis; middle temporal gyrus (MTG); superior frontal gyrus. The selection of these regions was primarily guided by prominent dual-stream models of auditory processing, which, in broad terms, propose that auditory information is processed in two streams: a ventral stream projecting from primary auditory areas on the supratemporal plane along anterior and middle temporal regions to inferior frontal cortex, and a dorsal stream projecting from primary areas along posterior temporal regions to parietal and superior frontal cortices (Friederici, 2011; Hickok and Poeppel, 2007; Rauschecker and Scott, 2009). We also included the insula as its functional connectivity has been previously studied as a function of musicianship (Zamorano et al., 2017).

Functional connectivity-behavior associations

We used regression analysis for relating behavioral measures of musical aptitude (AMMA total scores), tone-naming proficiency, and musical experience (age of onset of musical training, years of training, cumulative training) to the functional connectivity of the auditory ROIs. Separately for each behavioral measure, we performed voxel-wise regression of the functional connectivity maps with the respective behavioral measure as a single regressor using PALM (TFCE inference, 10,000 permutations, same search space as for the group comparisons). Musical aptitude can be sensibly measured in all participants (Gordon, 1989). However, tone naming requires knowledge on tone names, which non-musicians might not have, and measures of musical experience are only meaningful for musicians. Thus, we included all participants in the voxel-wise regression using the AMMA total scores but only included the musician groups for the regression using the tone-naming scores, age of onset, years of training, and cumulative training. The significance level was set to $\alpha = 0.05$, FWE-adjusted for multiple comparisons.

rsfMRI whole-brain graph-theoretical analysis

To assess effects of AP and musicianship on whole-brain functional connectivity, we used graph theory to characterize global differences in network topology between the groups. For each participant, we computed functional connectivity between all 96 parcels of the Harvard-Oxford cortical atlas (probability threshold = 25 %) using DPABI. Functional connectivity was quantified as Fisher's r-to-z-transformed Pearson correlation coefficients between the preprocessed, spatially averaged time-series of each parcel. This resulted in a 96 x 96 connectivity matrix per participant representing a whole-brain functional connectome comprising the individual parcels as nodes and the correlation coefficients as edges. Negative edges and edges from the diagonal of the connectivity matrices were set to zero (Power et al., 2010).

Whole-brain functional network topology was quantified using the graph-theoretical measures of *average strength*, *global efficiency*, *clustering coefficient*, *modularity*, and *(average) betweenness centrality* as implemented in the Brain Connectivity Toolbox (version 2019-03-03, https://sites.google.com/site/bctnet/) in MATLAB R2017b (Hallquist and Hillary, 2019; Rubinov and Sporns, 2010). *Average strength* characterizes how strongly the nodes are connected within a network and was defined as the mean of all node strengths. Node strength was computed by taking the sum of all edges of a node. *Global efficiency*, being inversely related to the *characteristic path length*, represents a measure of network integration and was computed as the mean inverse shortest path length in the network. The *clustering coefficient* is a measure of network segregation and was based on *transitivity*, which is the ratio of triangles to triplets in the network. *Modularity* describes the degree to which a network is subdivided into groups of nodes with a large number of within-module edges and a small number of between-module edges. The *(average) betweenness centrality* of the network was defined as the mean nodal betweenness centrality, which itself was computed based on the normalized number of all shortest paths in the network passing through a node.

For each participant, we proportionally thresholded and binarized the connectivity matrices using a wide range of thresholds from 35 % to 1 % retained edges in the network (in steps of 1 %). We then computed the above-listed measures for each threshold resulting in 35 values per measure and participant (*average strength* was based on non-binarized connectivity matrices). It is important to note that the type of thresholding employed in graph-theoretical analyses of brain networks (e.g., proportional or absolute thresholding) is subject to ongoing discussions (Hallquist and Hillary, 2019; van den Heuvel et al., 2017; Van Wijk et al., 2010). Absolute thresholding can lead to group differences in the number of edges in the networks which in turn causes spurious group differences in topology (Van Wijk et al., 2010). Proportional thresholding equates the number of edges in the network but has been criticized for being sensitive to overall differences in functional connectivity, especially in the presence of potentially random edges (van den Heuvel et al., 2017).

Group comparisons of whole-brain functional network topology

Group comparison of the graph-theoretical measures was performed using cluster-based permutation testing in R. Cluster-based permutation testing uses the dependency of graph-theoretical measures across thresholds to control the FWE rate and circumvents the choice of a single arbitrary threshold (Brauchli et al., 2020; Drakesmith et al., 2015; Langer et al., 2013; Maris and Oostenveld, 2007; Nichols and Holmes, 2002). We estimated the probability of clustered differences between the groups (i.e. across contiguous thresholds) under the null distribution. As before, we separately assessed the effects of AP (by comparing AP to RP musicians) and musicianship (by comparing RP to non-musicians). In addition, we replicated the potential effects of musicianship by comparing AP to non-musicians. In detail, we first conducted a two-sample Welch's *t*-test at each threshold. Second, we repeated the first step 5,000 times with permuted group labels. Crucially, we preserved the dependency across thresholds by keeping the random assignment of group labels identical across thresholds within one permutation. Third, we applied a (descriptive) cluster-defining threshold of $p < 0.05$ to build clusters of group differences. Finally, we compared the largest empirical cluster sizes k to the null distribution of cluster sizes derived from the permutations. The p-value was defined as the proportion of cluster sizes under the null distribution that was larger than or equal to k ($\alpha = 0.05$, FWE-adjusted across multiple thresholds).

Whole-brain functional network topology-behavior associations

We assessed associations between the graph-theoretical measures and the behavioral measures (AMMA total scores for all participants; tone-naming proficiency, age of onset, years of training, and cumulative training for the musician groups). For this, we computed the Pearson correlation coefficient (r) between the graph-theoretical measure averaged across all thresholds and the particular behavioral measure ($\alpha = 0.01$, Bonferroni-adjusted across multiple graph-theoretical measures).

rsfMRI whole-brain network-based statistic (NBS) analysis

To characterize local between-group differences in the whole-brain functional networks, we identified subnetworks differing between AP and RP musicians, between RP and non-musicians, and additionally between AP and non-musicians using two-sample *t*-tests as implemented in the network-based statistic (NBS) toolbox (version 1.2, https://sites.google.com/site/bctnet/comparison/nbs) (Zalesky et al., 2010). Analogous to cluster-based permutation testing, the NBS approach estimates the probability of group differences in subnetwork sizes under the null distribution and controls the FWE rate on the level of subnetworks. We used the following parameters: 5,000 permutations, test statistic = network extent, and subnetwork-defining thresholds; $t = 2.8$ for AP vs. RP, and RP vs. non-musicians; and $t = 3.4$ for AP vs. non-musicians. Statistically significant subnetworks were visualized using BrainNet Viewer (version 1.63, https://www.nitrc.org/projects/bnv/) (Xia et al., 2013).

rsfMRI whole-brain classification analysis

The analyses described in the previous paragraphs were (mass-)univariate in nature and thus sensitive for homogeneous increases and decreases in connectivity in one group relative to another. In contrast, multivariate approaches based on machine learning algorithms show high sensitivity for group differences in *patterns* of connectivity characterized by simultaneous increases and decreases (Haynes, 2015; Uddin et al., 2013). Thus, using multivariate pattern analysis (MVPA), we attempted to classify the participants into the three groups based on the individual whole-brain functional connectomes.

Group classification of the participants was performed with functions from scikit-learn (version 0.21.2, https://scikit-learn.org/) in Python 3.7.0. We first performed a multi-class classification into the three groups (AP, RP, non-musicians) using a "one-against-one"-approach with linear support vector machines (C = 1) as classifiers. For each participant, we extracted and flattened the upper right triangle of the connectivity matrix (excluding the diagonal) to build a 4,560-dimensional feature vector representing all edges in the whole-brain functional network. These vectors were associated with their respective group labels (AP, RP, non-musician) and stacked to build a dataset. We then z-transformed the dataset per feature and subsequently performed the classification of the participants into the groups. Classification accuracy was estimated using a 5-fold stratified cross-validation. Statistical significance of this accuracy was assessed by repeating the multi-class classification 5,000 times with permuted group labels. The *p*-value was defined as the proportion of accuracies derived from the permutations that were larger than or equal to the empirically obtained accuracy ($\alpha = 0.05$). To descriptively determine if a small number of features was sufficient for a successful classification, we used recursive feature elimination (RFE), which recursively prunes the least important feature (step = 1) to characterize accuracy as a function of the number of (informative) features (De Martino et al., 2008). The optimal number of features was determined using a 5-fold stratified cross-validation. Subsequently, we performed two follow-up classifications to differentiate AP from RP musicians and RP from non-musicians. The success of these classifications was quantified by classification accuracy, precision, and recall. We used the identical algorithm, cross-validation scheme, assessment of the statistical significance of the accuracy, and RFE as in the multi-class classification.

DWI ROI-to-ROI analysis

Based on the findings from the rsfMRI seed-to-voxel analyses, we next examined the interhemispheric *structural* connectivity between the left and the right PT in the three groups. First, we estimated diffusion parameters based on the preprocessed DWI data by fitting a diffusion tensor model at each voxel using *DTIFIT* in FSL. We specifically focused on two commonly investigated diffusion measures: fractional anisotropy (FA) and mean diffusivity (MD; computed as the mean of the three eigenvalues L1, L2, and L3) (Basser and Pierpaoli, 2011). Second, we individually reconstructed the white-matter pathways between the left and right PT using probabilistic tractography in FSL (default parameters unless otherwise stated). For this, we fitted a probabilistic diffusion model at each voxel using *BEDPOSTX* (Behrens et al., 2007,

2003). Probabilistic tractography was performed on the output of *BEDPOSTX* using *PROBTRACKX* (10,000 samples).

As in the rsfMRI analyses, the ROIs for the probabilistic tractography were based on atlases in MNI space. The seed and target ROIs for the bilateral PT were chosen based on the Harvard-Oxford atlas (probability threshold = 25 %). As a waypoint ROI, we used the midsagittal slice (3 mm thickness) of the corpus callosum map from the Jülich histological atlas (probability threshold = 10 %). As exclusion ROIs, we used the pre- and postcentral gyri as included in the Harvard-Oxford atlas (probability threshold = 25 %) to avoid false-positive pathways terminating in these brain regions. All ROIs were spatially dilated (5 mm spherical kernel) to increase the trackability of the pathways between them and to compensate for interindividual anatomical variability. Because probabilistic tractography was performed in participant-specific diffusion space, we computed the linear transformation from the individual diffusion space to the individual anatomical space using *flirt* and the nonlinear transformation from individual anatomical space to MNI space using *fnirt* in addition to *flirt*. Then, we concatenated these transformations using *convertwarp* and inverted the concatenated transformation using *invwarp*. The resulting warp fields (individual diffusion to MNI space and vice versa) were used in the tractography.

Third, we extracted FA and MD values from the *DTIFIT* output based on the pathways identified by the tractography, more specifically based on the sum of the connectivity distributions of pathways connecting the left PT to the right and vice versa. Before the extraction, we thresholded and binarized the connectivity distributions to retain the 3 % voxels with the highest probability per participant. The extracted FA and MD values were compared between AP and RP musicians, and RP and non-musicians using Welch's *t*-tests in R ($\alpha = 0.025$, Bonferroni-adjusted for multiple diffusion measures). Again, we also compared AP and non-musicians to replicate the potential effects of musicianship. We also associated the FA and MD values with the behavioral measures (AMMA total scores for all participants; tone-naming proficiency, age of onset, years of training, and cumulative training for the musician groups) using r ($\alpha = 0.025$).

DWI whole-brain graph-theoretical analysis

Analogously to the rsfMRI analyses, we assessed the effects of AP and musicianship on whole-brain structural connectivity. For this, we performed probabilistic tractography between all parcels of the Harvard-Oxford cortical atlas (probability threshold = 25 %) using *BEDPOSTX* and *PROBTRACKX* (5,000 samples). For each participant, this resulted in a 96 x 96 connectivity matrix representing a whole-brain structural connectome with the parcels as nodes and the connection probability between them as edges. Based on these connectivity matrices, we quantified and compared whole-brain structural network topology between AP and RP musicians, RP and non-musicians, and additionally between AP and non-musicians. All subsequent analysis steps were identical compared to the rsfMRI whole-brain graph-theoretical analysis (see above for details). We also performed the same correlations between the graph-theoretical measures and the behavioral measures as described above.

DWI whole-brain NBS analysis

We repeated the NBS analysis on the structural connectivity matrices to identify structural subnetworks differing between the groups. Apart from the subnetwork-defining threshold (here: $t = 2.7$ for AP vs. RP, and RP vs. non-musicians, and $t = 2.8$ for AP vs. non-musicians), we used identical parameters as in the rsfMRI analysis (see above for details).

DWI whole-brain classification analysis

We also performed the classification analysis based on the whole-brain structural networks. Apart from the different connectivity matrices, all analysis steps and parameters were identical to the rsfMRI whole-brain classification (see above for details).

Results

Behavioral results

Participant characteristics are given in Table 1. Group comparisons revealed no differences regarding age ($F(2,150) = 0.59$, $p = 0.55$, $BF_{01} = 9.30$, $\eta^2_G = 0.008$), movement during rsfMRI ($F(2,150) = 0.97$, $p = 0.38$, $BF_{01} = 6.75$, $\eta^2_G = 0.01$), and movement during DWI ($F(2,150) = 1.44$, $p = 0.24$, $BF_{01} = 4.54$, $\eta^2_G = 0.02$). Both musician groups showed substantially higher musical aptitude than non-musicians as measured by the AMMA total score; AP musicians vs. non-musicians: $t(85.22) = 8.48$, $p < 0.001$, $BF_{10} > 100$, $d = 1.69$; RP musicians vs. non-musicians ($t(91.17) = 6.54$, $p < 0.001$, $BF_{10} > 100$, $d = 1.30$). There was a trend towards a higher musical aptitude in AP musicians than in RP musicians ($t(99.12) = 1.99$, $p = 0.05$, $BF_{10} = 1.21$, $d = 0.39$), driven by higher AMMA tonal scores in AP musicians ($t(98.43) = 2.28$, $p = 0.02$, $BF_{10} = 2.05$, $d = 0.45$). The musician groups were comparable in the AMMA rhythm scores ($t(99.87) = 1.41$, $p = 0.16$, $BF_{01} = 1.98$, $d = 0.28$). With regard to tone-naming proficiency, AP musicians showed substantially higher tone-naming scores than RP musicians ($t(100.95) = 13.68$, $p < 0.001$, $BF_{10} > 100$, $d = 2.70$), and RP musicians showed better tone naming than non-musicians ($t(53.43) = 5.54$, $p < 0.001$, $BF_{10} > 100$, $d = 1.11$). The musician groups did not differ in their age of onset of musical training ($t(100.96) = -1.00$, $p = 0.32$, $BF_{01} = 3.08$, $d = 0.20$), years of musical training ($t(100.91) = 1.53$, $p = 0.13$, $BF_{01} = 1.71$, $d = 0.30$), and lifetime cumulative musical training ($t(96.81) = 1.13$, $p = 0.26$, $BF_{01} = 2.74$, $d = 0.22$).

Table 1. Participant characteristics.

Continuous measures are given as mean ± standard deviation. [+] Number of scans with framewise displacement (FD) ≥ 0.5 (Power et al., 2012). [$] Mean of average scan-to-scan translational (in mm) and rotational motion (in degrees) (Yendiki et al., 2014).

	AP musicians	**RP musicians**	**Non-musicians**
Number of participants	52	51	50
Sex (female / male)	24 / 28	24 / 27	24 / 26
Handedness (right / left / both)	45 / 4 / 3	46 / 4 / 1	44 / 6 / 0
Age	26.37 ± 4.98 years	25.29 ± 4.42 years	25.86 ± 5.52 years
rsfMRI movement [+]	8.90 ± 16.31 scans	5.61 ± 11.77 scans	5.26 ± 15.43 scans
DWI movement [$]	0.47 ± 0.11	0.48 ± 0.11	0.44 ± 0.12
Musical aptitude (AMMA) – total	66.04 ± 6.18	63.45 ± 6.96	52.80 ± 9.22
Musical aptitude (AMMA) – tonal	32.33 ± 3.67	30.55 ± 4.23	25.34 ± 5.02
Musical aptitude (AMMA) – rhythm	33.71 ± 2.78	32.90 ± 3.03	27.46 ± 4.58
Tone-naming score	76.41 ± 19.96 %	23.66 ± 19.16 %	8.41 ± 3.52 %
Age of onset of musical training	6.06 ± 2.40	6.53 ± 2.39	–
Years of musical training	20.31 ± 5.26 years	18.76 ± 5.01	–
Cumulative musical training	16,347.68 ± 12,582.35 hours	13,830.10 ± 9,985.04 hours	–

Abbreviations: AMMA = Advanced Measures of Music Audiation; AP = absolute pitch; DWI = diffusion-weighted imaging; FD = framewise displacement; RP = relative pitch; rsfMRI = resting-state functional magnetic resonance imaging.

Group differences in functional connectivity of auditory ROIs

To assess the effects of AP and musicianship on the functional connectivity of the auditory ROIs, we compared the functional connectivity maps between AP and RP musicians, and between RP musicians and non-musicians (the minimal FWE-corrected *p* values per cluster [p_{FWE}] and cluster sizes [*k*] are given in brackets). Group comparisons between AP musicians and RP musicians revealed no significant clusters for any of the four auditory seed ROIs (all $p_{FWE} > 0.05$). Comparisons between RP musicians and non-musicians revealed that RP musicians showed increased interhemispheric functional connectivity between the left PT (seed ROI) and a cluster in the right PT ($p_{FWE} = 0.02$, $k = 47$; see Figure 1A). A subset of this cluster also survived additional correction across the four ROIs ($p_{FWE\text{-}ROI\text{-}corr.} = 0.04$, $k = 7$). We also identified differences in the symmetric functional connection between the right PT (seed ROI) and two clusters in the left PT ($p_{FWE} = 0.03$, $k = 51$ and $p_{FWE} = 0.04$, $k = 8$). These clusters did not survive additional correction across ROIs (minimum $p_{FWE\text{-}ROI\text{-}corr.} = 0.08$). Details on the clusters are given in Table 2.

Table 2. Significant group differences between RP musicians and non-musicians in the rsfMRI seed-to-voxel analysis.

Coordinates (x, y, z) of voxels with minimum *p* values are in MNI space. Clusters are ordered according to seed region and size.

Contrast	Seed region	Target region	*k*	p_{FWE}	x	y	z
RP > Non-mus	Left PT	Right PT	47	0.02	63	-18	9
RP > Non-mus	Right PT	Left PT	51	0.03	-54	-27	3
RP > Non-mus	Right PT	Left PT	8	0.04	-39	-36	9

Abbreviations: Non-mus = non-musicians; *k* = cluster size in voxels; p_{FWE} = minimal family-wise error-corrected *p* value in cluster; PT = planum temporale; RP = relative pitch.

As we did not find evidence for group differences between AP and RP musicians in the functional connectivity of the auditory ROIs, we attempted to replicate the effects of musicianship that we identified via the comparison of RP and non-musicians. For this, we compared the functional connectivity maps between AP musicians and non-musicians. These comparisons revealed that AP musicians also showed increased interhemispheric functional connectivity between the left and right auditory regions (see Supplementary Table 1). Overall, these clusters were descriptively larger in number and size, and observable from more seed regions (see Supplementary Figure 1).

Associations between functional connectivity and behavior

Using voxel-wise regression analysis, we related tone-naming proficiency, musical aptitude, and musical experience to the functional connectivity of the auditory ROIs. Within musicians, higher tone-naming proficiency was associated with increased functional connectivity between the right HG (seed ROI) and surrounding regions including the posterior insula and associative auditory areas (p_{FWE} = 0.02, k = 242). Most voxels of this cluster also survived additional correction across ROIs ($p_{FWE\text{-}ROI\text{-}corr.}$ = 0.03, k = 152). Across all participants, we found that higher musical aptitude as measured by the AMMA total scores were associated with increased functional connectivity within the left PT (p_{FWE} = 0.04, k = 5). Furthermore, we unexpectedly observed that higher musical aptitude was associated with lower functional connectivity between the left HG (seed ROI) and a cluster in the left MTG (p_{FWE} = 0.04, k = 6). Both of these clusters were very small in size ($k < 10$) and did not survive additional correction across ROIs. Within the musician groups, lower age of onset of musical training was associated with increased functional connectivity between the right HG (seed ROI) and a cluster in the right dorsolateral prefrontal cortex (DLPFC) (p_{FWE} = 0.02, k = 46). This cluster did not survive additional correction for multiple ROIs. We further found that a lower age of onset was associated with increased functional connectivity between the right planum temporale (seed ROI) and the right DLPFC (p_{FWE} = 0.03, k = 23). A subset of this cluster just survived additional correction for multiple ROIs ($p_{FWE\text{-}ROI\text{-}corr.}$ = 0.046, k = 6). Finally, we found no evidence for an association between years of training or cumulative training and the functional connectivity of the auditory ROIs (all $p_{FWE} > 0.05$). Significant associations within musicians are depicted in Figure 1B and across all subjects in Figure 1C.

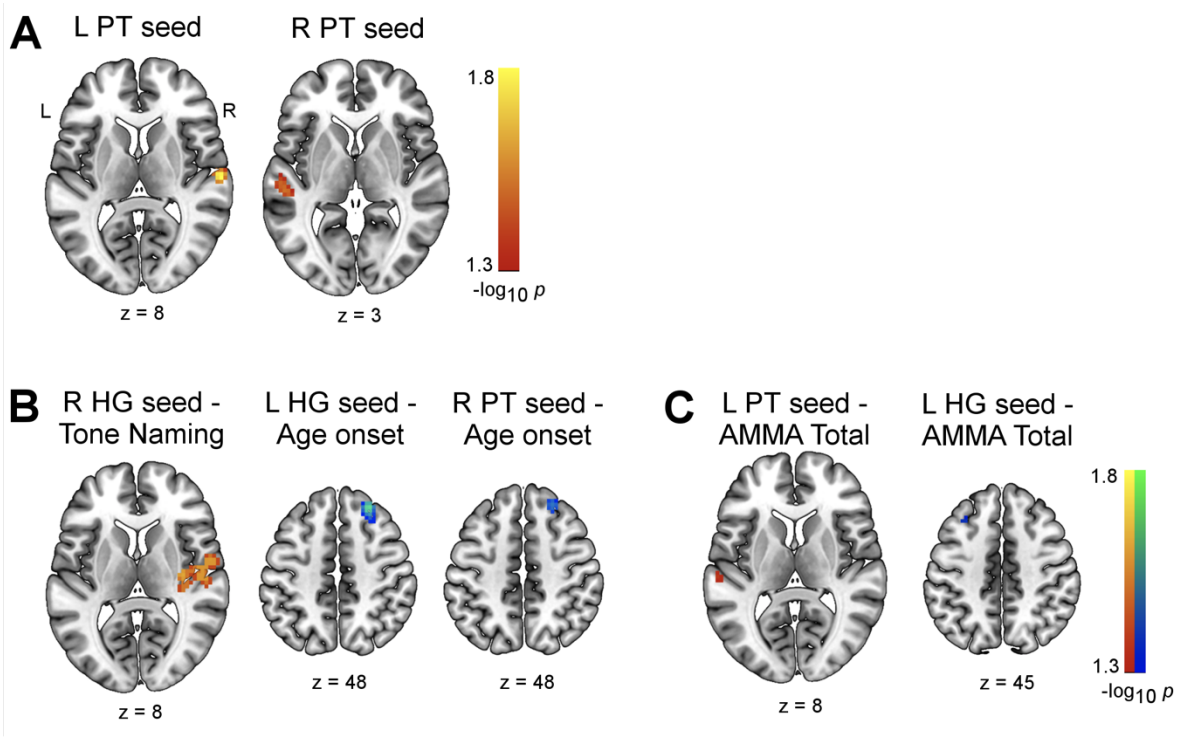

Figure 1.

A) Increased intrinsic functional connectivity between left and right PT in RP musicians compared to non-musicians ($p_{FWE} < 0.05$). B) Associations between functional connectivity and behavior in musicians and C) across all subjects ($p_{FWE} < 0.05$). Abbreviations: AMMA = Advanced Measures of Music Audiation; HG = Heschl's gyrus; L = left; PT = planum temporale; R = right.

Table 3. Significant voxel-wise functional connectivity-behavior associations.

Coordinates (x, y, z) of voxels with minimum *p* values are in MNI space. Clusters are ordered according to behavioral measures and signs of the association.

Behavior	**Seed region**	**Target region**	**Sign**	***k***	p_{FWE}	**x**	**y**	**z**
Tone naming	Right Heschl's gyrus	Right posterior insula, auditory association areas	+	242	0.02	36	-15	15
AMMA total	Left PT	Left PT	+	5	0.04	-60	-24	9
AMMA total	Left Heschl's gyrus	Left MTG	-	6	0.04	-30	24	48
Age onset	Right Heschl's gyrus	Right DLPFC	-	46	0.02	27	36	48
Age onset	Right PT	Right DLPFC	-	23	0.03	24	36	48

Abbreviations: AMMA = Advanced Measures of Music Audiation; DLPFC = dorsolateral prefrontal cortex; *k* = cluster size in voxels; MTG = middle temporal gyrus; p_{FWE} = minimal family-wise error-corrected p-value in cluster; PT = planum temporale; + = positive association; - = negative association.

Group differences in functional network topology

Group comparisons of whole-brain functional network topology revealed the following results (FWE-corrected *p* values per cluster [p_{FWE}] and cluster size across contiguous thresholds [*k*] are given in brackets). We found no evidence for group differences between AP and RP musicians in any of the investigated graph-theoretical measures (all $p_{FWE} > 0.05$). However, we observed an effect of musicianship on multiple graph-theoretical measures: We found higher *average strength* ($p_{FWE} = 0.01$, $k = 35$), lower *global efficiency* ($p_{FWE} = 0.04$, $k = 11$), and a higher *clustering coefficient* ($p_{FWE} = 0.01$, $k = 25$) in RP musicians than in non-musicians (see Figure 2A). We found no evidence for an effect of musicianship on *modularity*, and *betweenness centrality* of whole-brain functional networks (both $p_{FWE} > 0.05$). Strikingly similar results were obtained by comparing AP and non-musicians, replicating the effects of musicianship on functional network topology (see Supplementary Table 2 for details).

Associations between functional network topology and behavior

We found no evidence for an association between *average strength*, *clustering coefficient*, *modularity*, or *betweenness centrality* and any of the behavioral measures for musical aptitude, tone-naming proficiency, or musical experience (all $p > 0.01$ [$\alpha = 0.01$, adjusted for multiple graph-theoretical measures]). There was a significant negative correlation between *global efficiency* and the AMMA total scores across all participants ($r = -0.23$, $p = 0.004$). However, this correlation was likely driven by group differences in both measures as we found no evidence for a correlation within AP musicians ($r = 0.01$, $p = 0.90$), RP musicians ($r = -0.21$, $p = 0.14$), or non-musicians ($r = -0.11$, $p = 0.49$). For all other behavioral measures, we found no evidence for an association with *global efficiency* (all $p > 0.01$).

Group differences in whole-brain functional subnetworks

The whole-brain NBS analysis to reveal functional subnetworks differing between the groups did not show evidence for differences between AP and RP musicians ($p_{FWE} > 0.05$). In contrast, we identified a subnetwork characterized by higher functional connectivity in RP musicians than in non-musicians ($p_{FWE} = 0.04$). As shown in Figure 2B, the descriptively strongest group differences within this subnetwork were present in interhemispheric functional connections between the left and right PT; between the left IFG,po and the right pSTG; between left and right pSTG; and between the left and right IFG,po. Additional nodes of this functional subnetwork were located in brain regions of the temporal and parietal lobes, including HG and anterior and posterior SMG. Detailed information on all nodes and edges of the functional subnetwork differing between RP and non-musicians are given in Supplementary Table 3. In the internal replication of these effects of musicianship, we found a strikingly similar subnetwork differing between AP musicians and non-musicians ($p_{FWE} = 0.005$). This functional subnetwork is visualized in Supplementary Figure 2A, and details regarding all nodes and edges are given in Supplementary Table 4.

Functional network-based classification

Group classification based on whole-brain functional networks using MVPA yielded the following results: The multi-class classification successfully classified the participants into the three groups with an accuracy of 47 %, $p = 0.002$ (chance level = 33 %). See Supplementary Figure 3A for a visualization of the null distribution of accuracies with permuted group labels. According to RFE, the optimal number of features for classification was quite large (604 edges), which suggests that the connectivity patterns of a substantial part of the whole-brain functional network contained information about group membership. The confusion matrix showed that the classifier confused AP and RP musicians most often, but participants of the musician groups were less often classified as non-musicians and vice versa (see Supplementary Figure 3B). Consistent with this pattern of results, the follow-up classification within musicians showed that AP and RP musicians could not be successfully differentiated (accuracy = 57 %, $p = 0.12$ [chance level = 50%], precision = 0.56, recall = 0.6; see Supplementary Figure 3C). In contrast, the classification of RP musicians and non-musicians was successful (accuracy = 65 %, $p = 0.01$ [chance level = 50%], precision = 0.7, recall = 0.6; see Supplementary Figure 3D). The optimal number of features necessary for successful classification was again relatively high (1,422 edges).

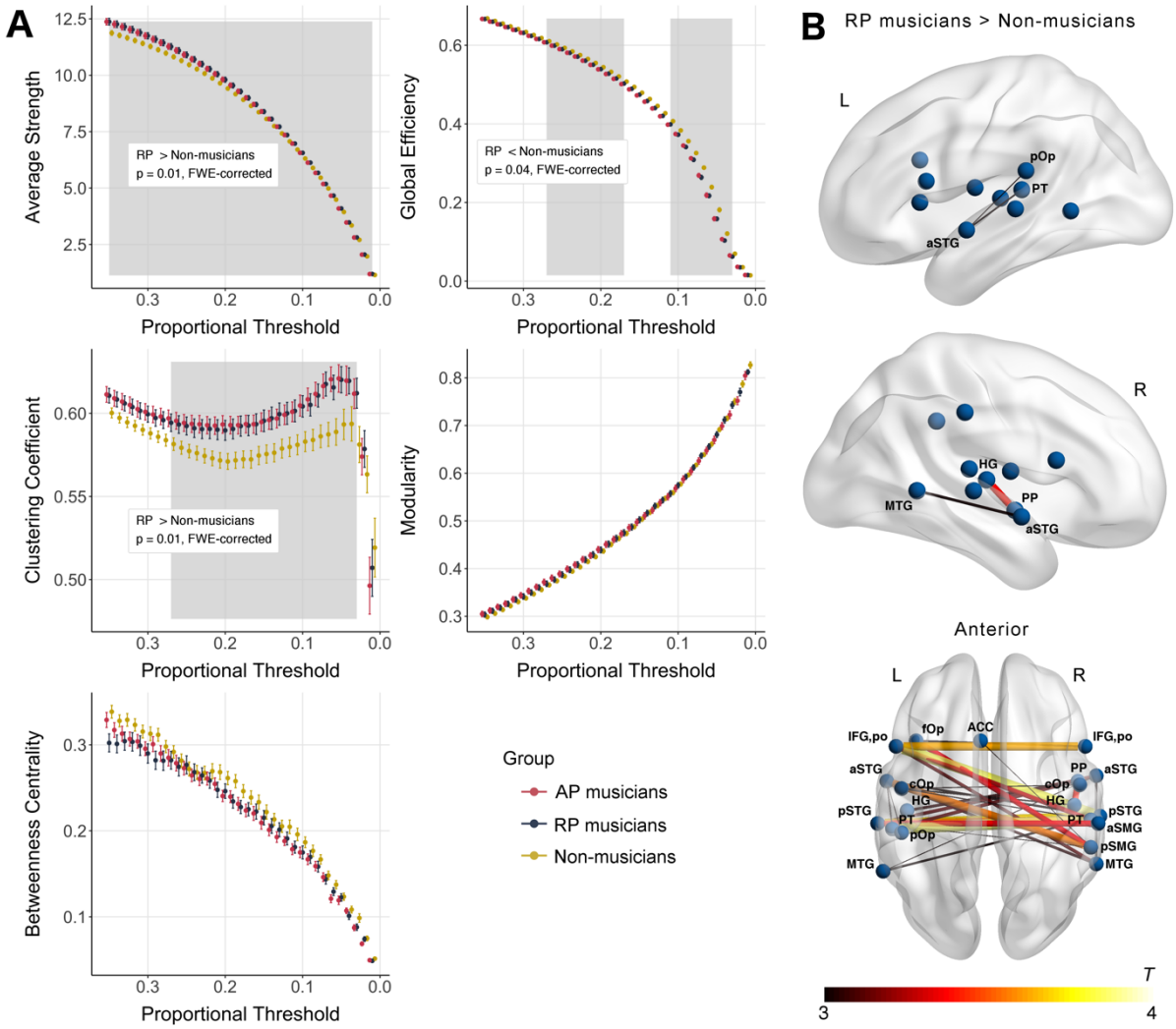

Figure 2.

A) Group differences between RP musicians and non-musicians in graph-theoretical measures calculated based on whole-brain functional networks ($p_{FWE} < 0.05$). Gray-shaded area indicates range of thresholds belonging to statistically significant cluster. B) Subnetwork with increased functional connectivity in RP musicians compared to non-musicians obtained in the NBS analysis ($p_{FWE} < 0.05$). Abbreviations: ACC = anterior cingulate cortex; AP = absolute pitch; aSMG = anterior supramarginal gyrus; aSTG = anterior superior temporal gyrus; cOp = central operculum; fOp = frontal operculum; HG = Heschl's gyrus; IFG,po = inferior frontal gyrus, pars opercularis; L = left; MTG = middle temporal gyrus; pSTG = superior temporal gyrus, posterior division; pOp = parietal operculum; PT = planum temporale; R = right; RP = relative pitch.

Group differences in transcallosal structural connectivity

In nine AP musicians, 14 RP musicians, and 15 non-musicians, probabilistic tractography was not able to identify a white-matter pathway connecting left and right PT (see Figure 3C for a visualization of the white-matter tract). Consequently, these participants were excluded from group comparisons of transcallosal connectivity and the structural connectivity-behavior correlations. Results of the group comparisons of transcallosal structural connectivity are visualized in Figure 3A. We found no evidence for group differences

in FA between AP musicians and RP musicians ($t(68.34) = 0.81$, $p = 0.42$, $d = 0.19$), and between RP musicians and non-musicians ($t(69.17) = 0.12$, $p = 0.90$, $d = 0.03$). Furthermore, there was no evidence for differences in MD between AP and RP musicians ($t(70.02) = -1.01$, $p = 0.31$, $d = 0.23$). On the contrary, we found a significant difference in MD between RP and non-musicians, characterized by higher MD values in RP than in non-musicians ($t(59.51) = 2.61$, $p = 0.01$, $d = 0.61$). In the internal replication of this effect of musicianship, we found that AP musicians descriptively showed higher MD values than non-musicians, but this difference did not reach statistical significance ($t(75.11) = 1.81$, $p = 0.07$ [$\alpha = 0.025$, adjusted for multiple diffusion measures], $d = 0.40$).

Associations between transcallosal structural connectivity and behavior

Structural connectivity-behavior associations are shown in Figure 3B. Across both musician groups, we found a significant negative correlation between the age of onset of musical training and FA values within the pathway connecting left and right PT ($r = -0.28$, $p = 0.01$). We did not find evidence for an association between any of the other behavioral measures and FA (all $p > 0.025$). Furthermore, we found a significant positive correlation between age of onset and MD values across both musician groups ($r = 0.31$, $p = 0.005$). Again, there was no evidence for an association of any of the other behavioral measures and MD (all $p > 0.025$).

Group differences in structural network topology

In the analysis of whole-brain structural network topology, we found no evidence for group differences between AP musicians and RP musicians, or between both musician groups and non-musicians in any of the investigated graph-theoretical measures (all $p_{FWE} > 0.05$).

Associations between structural network topology and behavior

We found a significant positive correlation between *betweenness centrality* and the musicians' age of onset of musical training ($r = 0.27$, $p = 0.006$). Furthermore, age of onset was also descriptively associated with *mean strength* ($r = -0.19$, $p = 0.049$), *global efficiency* ($r = -0.21$, $p = 0.04$), and *clustering coefficient* ($r = 0.22$, $p = 0.02$; see Figure 4A). However, these correlations did not survive the adjustment of the significance level for multiple graph-theoretical measures. We found no evidence for an association of *modularity* and age of onset. Furthermore, there was no evidence for an association between any of the other behavioral measures (besides age of onset) and the graph-theoretical measures.

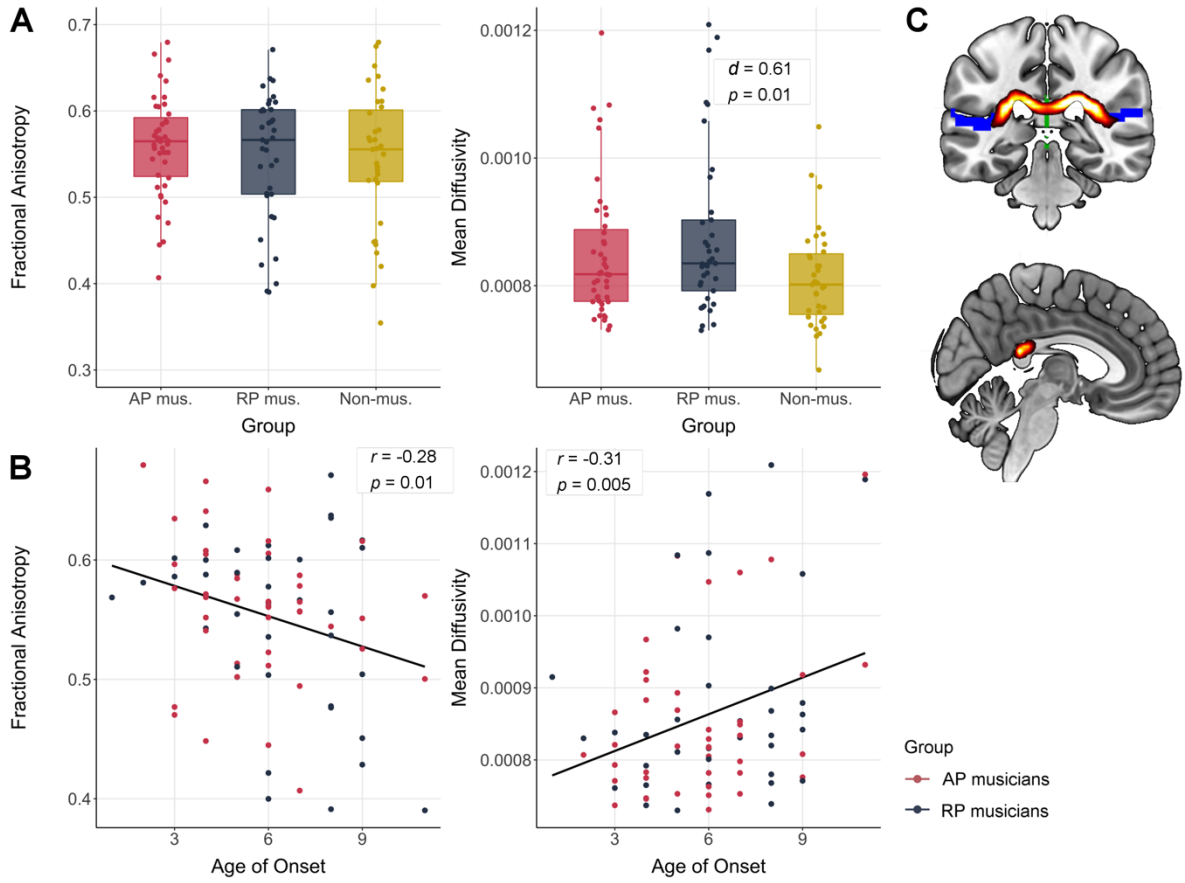

Figure 3.

A) Group differences between AP, RP, and non-musicians in fractional anisotropy and mean diffusivity values (α = 0.025, adjusted for multiple diffusion measures). B) Associations between fractional anisotropy and mean diffusivity values and age of onset of musical training. C) Coronal and sagittal view of the mean white-matter pathway between left and right PT obtained by probabilistic tractography across all subjects. Abbreviations: AP = absolute pitch; Non-mus = non-musicians; PT = planum temporale; RP = relative pitch.

Group differences in whole-brain structural subnetworks

As for the functional data, the NBS analysis to identify structural subnetworks differing between the groups did not show evidence for differences between AP musicians and RP musicians ($p_{FWE} > 0.05$). On the contrary, we again identified a subnetwork characterized by higher structural connectivity in RP than in non-musicians ($p_{FWE} = 0.047$). As can be seen from Figure 4B, the descriptively biggest group difference in structural connectivity was between the posterior cingulate cortex (PCC) and the frontal pole (FP). Furthermore, RP musicians showed higher structural connectivity between right perisylvian regions including the parietal operculum (pOp) as well as preCG and postCG. Detailed information on all nodes and edges of the structural subnetwork differing between RP and non-musicians are given in Supplementary Table 5. A similar subnetwork was identified by comparing AP and non-musicians ($p_{FWE} = 0.003$). This subnetwork had descriptively stronger group differences and was more extended than the subnetwork identified by comparing RP and non-musicians. This structural subnetwork is visualized in Supplementary Figure 2B, and details regarding all nodes and edges are given in Supplementary Table 6.

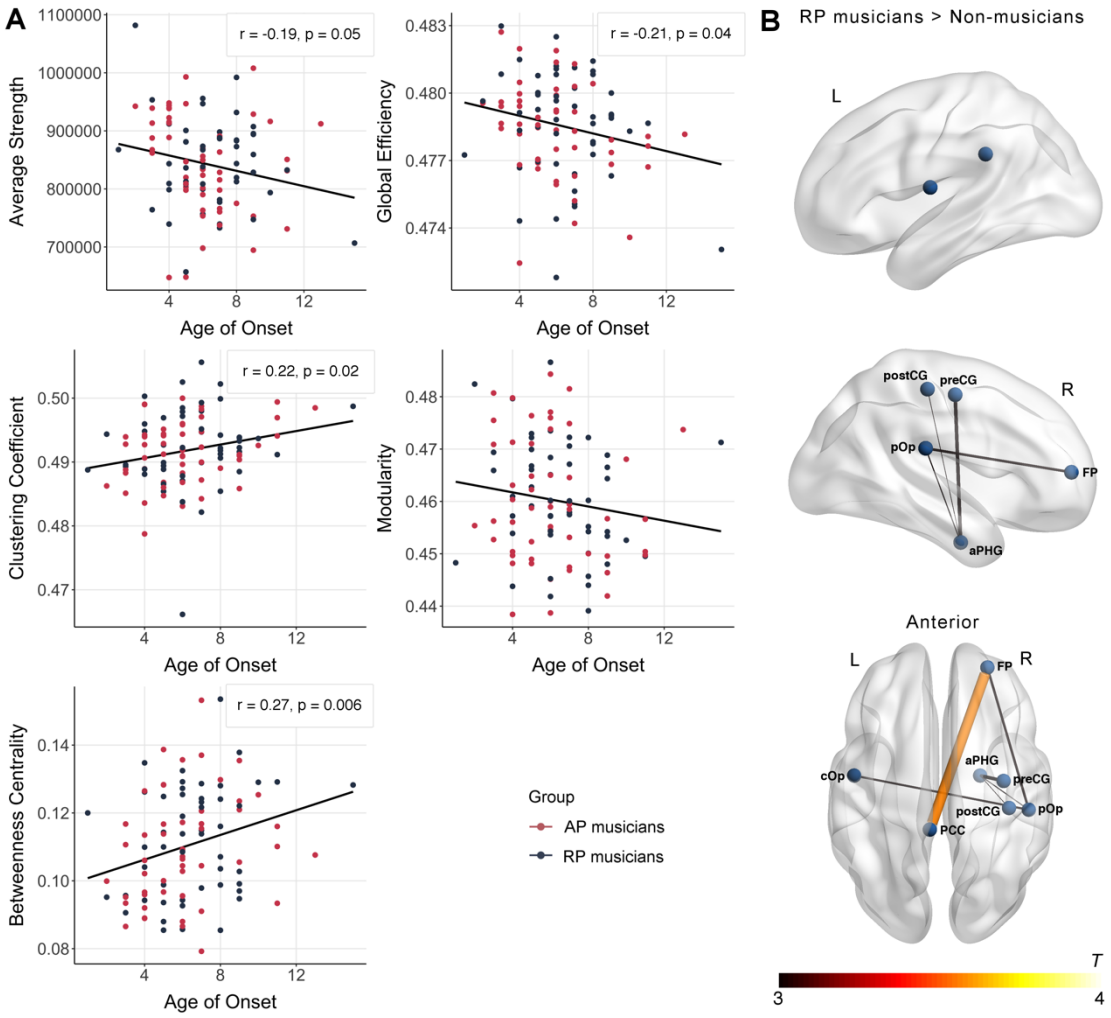

Figure 4.

A) Associations between structural network topology and age of onset of musical training for AP- and RP musicians. B) Subnetwork with increased structural connectivity in RP musicians compared to non-musicians obtained in the NBS analysis ($p_{FWE} < 0.05$). Abbreviations: aPHG = anterior parahippocampal gyrus; cOp = central operculum; FP = frontal pole; PCC = posterior cingulate cortex; postCG = postcentral gyrus; preCG = precentral gyrus; pOp = parietal operculum; PT = planum temporale; R = right.

Structural network-based classification

Group classification based on whole-brain structural networks using MVPA yielded no successful classifications. The three groups could not be successfully differentiated in the multi-class classification (accuracy = 35 %, p = 0.33 [chance level = 33 %]). Furthermore, the follow-up classifications showed that neither RP and AP musicians (accuracy = 43 %, p = 0.90 [chance level = 50%], precision = 0.41, recall = 0.49), nor RP and non-musicians (accuracy = 52 %, p = 0.35 [chance level = 50%], precision = 0.53, recall = 0.52) could be successfully differentiated.

Table 4. Summary of main findings for group comparisons, classifications, and brain-behavior associations.

	RP vs. Non-mus	AP vs. Non-mus	AP vs. RP
Functional connectivity of auditory ROIs	RP musicians show increased interhemispheric functional connectivity between the left and right PT	AP musicians show increased interhemispheric functional connectivity between the left and right auditory cortex (PT and HG), and between bilateral auditory cortex and right inferior frontal regions	No statistical evidence for group differences
Associations between functional connectivity of auditory ROIs and behavior	Positive association between tone-naming proficiency and functional connectivity of the right HG and associative auditory areas within musicians; negative association between age of onset and functional connectivity between right PT and right DLPFC within musicians		
Functional network topology	RP musicians show higher average strength and cluster coefficient, and a lower global efficiency	AP musicians show higher average strength and cluster coefficient, and a lower global efficiency	No statistical evidence for group differences
Functional subnetworks	RP musicians show increased functional connectivity within subnetwork consisting of bilateral auditory cortex, bilateral inferior frontal cortex, anterior and middle temporal cortex, and inferior parietal cortex	AP musicians show increased functional connectivity within subnetwork consisting of bilateral auditory cortex, right inferior frontal cortex, left anterior temporal cortex, and inferior parietal cortex	No statistical evidence for group differences
Functional network-based classification	Statistically significant classification	-	No evidence for successful classification
Structural connectivity of auditory ROIs	RP musicians show increased mean diffusivity in transcallosal white-matter tract connecting left and right PT	AP musicians descriptively show a trend towards increased mean diffusivity in transcallosal white-matter tract connecting left and right PT	No statistical evidence for group differences
Association between structural connectivity of auditory ROIs and behavior	Negative association between age of onset of musical training and FA values and positive association with MD values of white-matter tract between left and right PT within musician groups		
Structural network topology	No statistical evidence for group differences	No statistical evidence for group differences	No statistical evidence for group differences
Association between structural network topology and behavior	Positive association between age of onset and betweenness centrality in musicians		
Structural subnetworks	RP musicians show increased structural connectivity within a subnetwork consisting of right-hemispheric sensorimotor (preCG, postCG), medial temporal, and frontal cortex as well as bilateral perisylvian regions	AP musicians show increased structural connectivity within a subnetwork consisting of right-hemispheric sensorimotor (preCG, postCG), inferior temporal, and frontal cortex, as well as bilateral insular cortex and bilateral perisylvian regions	No statistical evidence for group differences
Structural network-based classification	No evidence for successful classification	-	No evidence for successful classification

Abbreviations: AP = absolute pitch; DLPFC = dorsolateral prefrontal cortex; FA = fractional anisotropy; HG = Heschl's gyrus; MD = mean diffusivity; Non-mus = non-musicians; preCG = precentral gyrus; postCG = postcentral gyrus; PT = planum temporale; ROI = region of interest; RP = relative pitch.

Discussion

In this study, we assessed the effects of musicianship and AP on functional and structural large-scale brain networks. Our main results are summarized in Table 4. We found robust effects of musicianship across various methodological approaches, which were largely replicable in two separate groups of AP and RP musicians. Both musician groups showed stronger interhemispheric functional connectivity between left and right PT, enhanced connectivity in temporal-parietal-frontal functional subnetworks, and globally altered functional network topology, compared to non-musicians. Furthermore, RP musicians and non-musicians could be successfully classified using MVPA based on whole-brain functional connectomes. Musicians also showed altered transcallosal structural connectivity in the white-matter tract connecting bilateral PT. We detected several brain-behavior associations between connectivity and behavioral measures of musicianship, most prominently between structural network features and the age of onset of musical training. Finally, we found no evidence for group differences between RP and AP musicians across all analyses: the two musician groups showed striking similarities in both functional and structural networks. In the following discussion, we integrate these comprehensive results and relate them to evidence from previous studies on the effects of musicianship and AP on functional and structural connectivity.

A main finding of this study is the altered functional and structural connectivity between left and right PT in both musician groups compared to non-musicians. Consistent with our probabilistic tractography results, auditory areas in the superior temporal lobes of the two hemispheres are structurally connected via fibers in the isthmus and splenium of the corpus callosum (Hofer and Frahm, 2006; Witelson, 1989). Whereas effects of musicianship on (more anterior) parts of the corpus callosum connecting bilateral motor areas have been frequently observed (Bengtsson et al., 2005; Öztürk et al., 2002; Schlaug et al., 2009, 1995; Schmithorst and Wilke, 2002; Vollmann et al., 2014), only one previous study has reported microstructural differences between musicians and non-musicians in the callosal fibers connecting the left and right PT (Elmer et al., 2016). Here, we showed that the altered microstructural connectivity is accompanied by increased intrinsic functional connectivity in musicians, an observation that substantiates earlier reports of increased functional connectivity between bilateral auditory areas using low-resolution electroencephalography (EEG) source estimation (Klein et al., 2016). The PT is located immediately posterior to HG on the superior temporal plane, and its important role in auditory processing is well documented (Griffiths and Warren, 2002). One interpretation of increased interhemispheric functional connectivity in musicians is an increased information transfer and coordination between the two areas across both hemispheres (van der Knaap and van der Ham, 2011). It is conceivable that an enhancement in coordinating information extracted from sounds is the basis for the superior auditory skills frequently noted in musically trained individuals (Kraus and Chandrasekaran, 2010). Musicians show extensive and precise neural processing of basic acoustic features such as pitch (Schneider et al., 2002; Wong et al., 2007), timbre (Pantev et al., 1998), and the extraction of these features from complex acoustic signals such as speech and music (Chartrand and Belin, 2006; Magne et al., 2006).

Regarding functional networks, the effects of musicianship were not restricted to interhemispheric auditory-to-auditory connections: We identified widespread subnetworks showing enhanced connectivity in musicians, mostly encompassing bilateral superior and middle temporal, inferior frontal, and inferior parietal regions. These regions can be well situated within the frameworks of dual-stream models for auditory processing (Friederici, 2011; Hickok and Poeppel, 2007; Rauschecker and Scott, 2009). In particular, our data suggest that communication between regions of the bilateral ventral stream is shaped by musicianship more strongly than that between regions of the dorsal stream (see Figure 2). However, most altered connections in the subnetwork were of interhemispheric nature. It has been shown that interhemispheric information transfer causally modulates expansive auditory and motor networks during rest (Andoh et al., 2015). Thus, experience-dependent plasticity in interhemispheric connections could have a prime role in modulating network interactions between auditory areas and cortical regions in the temporal, parietal, and frontal lobes. With regard to reproducibility, we did not detect alterations in the connectivity of many brain regions that have previously been associated with musicianship such as the visual cortex (Luo et al., 2012), insular cortex (Zamorano et al., 2019, 2017), or the orbitofrontal cortex (Fauvel et al., 2014). As we were able to replicate virtually the same enhanced subnetworks in both RP and AP musicians compared to non-musicians, the identified subnetworks of the current study seem to robustly reflect general characteristics of musical expertise. Finally, these networks show a high similarity with the subnetworks identified in a previous study of our group using EEG (Klein et al., 2016), which suggests that potential influences of the noisy rsfMRI acquisition on the intrinsic functional networks are negligible.

A notable feature of the DWI results is the consistent and highly specific association between the age of onset of musicians training and structural network measures. Importantly, these network measures were not associated with other behavioral measures such as cumulative training hours and years of training. First, age of onset of musical training was correlated with diffusion measures in the transcallosal white-matter tract connecting left and right PT. This result complements previous reports of associations between age of onset and diffusion measures in parts of the corpus callosum connecting bilateral sensorimotor brain regions (Steele et al., 2013). These fibers are located rostrally adjacent to the callosal fibers investigated in this study. An earlier study also showed an association of age of onset with diffusion measures of both the anterior and the posterior part of the corpus callosum (Imfeld et al., 2009). These findings, together with the results of the current study, suggest that microstructural properties of the corpus callosum are sensitive for changes when musical training starts at a young age, possibly during a sensitive period when the potential for plasticity is especially high (Penhune, 2011; Schlaug et al., 1995). Second, for the first time, we observed associations between of age of onset and whole-brain structural network topology. Thus, musical training during early childhood not only has local effects on microstructure, but also has global effects on the topology of the structural connectome, and these effects are stronger the earlier musical training begins.

This is the first study to analyze effects of musicianship on both structural and functional connectivity in a multimodal dataset consisting of fMRI and DWI data. In this context, one particular aspect of our results

warrants further discussion, namely that although we found effects in both modalities, the correspondence between effects of musicianship on functional versus structural networks was surprisingly low. Previous evidence suggests that intrinsic functional connectivity (as measured using rsfMRI) and the presumed underlying structural connectivity (as measured using DWI) are to some extent related, at least for selected large-scale brain networks, such as the default-mode network (Greicius et al., 2009), or for a subset of connections between brain regions (Hermundstad et al., 2013). However, due to the presence of indirect structural connections, functional connectivity between regions can also be observed without direct structural links (Damoiseaux and Greicius, 2009; Honey et al., 2009). We found that effects of musicianship on connectivity were particularly strong in the functional domain, and less so in the structural domain. Therefore, based on our data, one might speculate that musical training more strongly shapes functional networks, and does so mostly independently of structural networks. An important exception to this general observation concerns the observed differences in transcallosal connectivity between bilateral PT. However, this selective correspondence is highly consistent with the finding that interhemispheric functional connectivity causally depends on structural connectivity provided via the corpus callosum (Jäncke and Steinmetz, 1998, 1994; Roland et al., 2017). Apart from the extent of the effects, there is also a disparity in the scale of the effects of musicianship on connectivity. Whereas functional effects were present across both local and global analyses, structural effects were restricted to a small number of local connections. The importance of functional adaptations associated with musical training is also emphasized by the result that musicians and non-musicians could only be successfully classified based on functional but not based on structural whole-brain connectomes, and the successful classification relied on a large number of functional connections, as demonstrated by the RFE algorithm.

A common theme across all rsfMRI and DWI analyses was the remarkable similarity of intrinsic functional and structural networks between the two musician groups. For example, graph-theoretical measures representing functional network topology were almost identical across a wide range of thresholds (see Figure 2). Using highly sensitive MVPA, the musician groups could not be classified based on whole-brain functional or structural connectomes. The lack of detectable differences between AP and RP musicians seems somewhat surprising, given that previous studies have reported various effects of AP on functional and structural connectivity when compared to RP musicians. However, there are multiple reasons potentially contributing to this discrepancy. First, previous evidence for the effects of AP on connectivity is sparse: the number of studies reporting differences in intrinsic functional (Brauchli et al., 2019; Elmer et al., 2015; Kim and Knösche, 2017) and structural connectivity (Burkhard et al., 2020; Dohn et al., 2015; Kim and Knösche, 2016; Loui et al., 2011; Oechslin et al., 2010a) is relatively small, none of the effects have been replicated within a single study or by an independent study to date, and the effects reported were very subtle in size. Second, all but the two studies having an overlap with the participants of the current study (Brauchli et al., 2019; Burkhard et al., 2020) investigated small to very small samples, making them prone to false-positive results (Button et al., 2013). Third, a large variety of different modalities and various methods of analysis have been employed in previous studies. Apart from conventional univariate rsfMRI (Kim and Knösche, 2017) and DWI analyses (Dohn et al., 2015), these range from ROI-based EEG source

estimation analyses (Elmer et al., 2015) to MVPA-based rsfMRI analyses of local and global connectivity (Brauchli et al., 2019), to intracortical myelination analyses of anatomical MRI images (Kim and Knösche, 2016). Fourth, defining AP is not straightforward as there is no agreement on whether AP musicians represent a distinct population (Athos et al., 2007) or merely lie on the upper end of a continuum of tone-naming abilities (Bermudez and Zatorre, 2009). In accordance with many previous studies, we defined AP based on self-report, which was confirmed using a tone-naming test. Due to the lack of a gold standard, tone-naming tests in AP research differ considerably in procedure (e.g., stimulus type [sine tones or instrumental tones], trial duration, response window, and registration), the number of stimuli, and the presentation technique (e.g., online or laboratory-based). Furthermore, no cutoff in tone-naming scores has been established to differentiate between AP and RP musicians. The AP and RP musicians of our study strongly differed from each other in terms of the tone-naming proficiency ($d > 2$). Combined with our large sample, this suggests that a difference in intrinsic functional and structural networks would have been identified if a meaningful difference existed. Thus, we are confident that the lack of differences between AP and RP musicians is a valid finding, given the methodology and sample size employed here. In this context, it is important to note that our results should not be regarded as evidence that there are no brain differences between AP and RP musicians. Task-based studies designed to investigate the tone labeling ability of AP musicians in action have shown considerable promise for uncovering the neural peculiarities of the phenomenon (Greber et al., 2018; Leipold et al., 2019b, 2019c; McKetton et al., 2019; Schulze et al., 2013; Wengenroth et al., 2014).

To conclude, we identified robust effects of musical expertise on intrinsic functional and structural large-scale brain networks, which were largely replicable in two musician groups. Whereas effects were especially prominent in interhemispheric connections between bilateral auditory areas, we also found enhanced connectivity in temporal-parietal-frontal functional subnetworks, and globally altered functional network topology associated with musicianship. As effects were stronger in the functional domain, we speculate that musical training particularly affects functional brain networks compared to structural networks. We did not find evidence for an effect of AP on functional or structural connectivity. Differences between AP and RP musicians might be extremely subtle, and thus require very large samples or task-based experiments to be detected.

Acknowledgments

This work was supported by the Swiss National Science Foundation (SNSF), grant no. 320030_163149 to LJ. We are extremely grateful to Désirée Yamada for her invaluable help in data acquisition and research administration. We also thank Silvano Sele for his support with the statistical analyses and Marielle Greber for her helpful comments on an earlier version of this manuscript.

Conflicts of Interest

The authors declare no conflicts of interest.

References

Abdul-Kareem IA, Stancak A, Parkes LM, Al-Ameen M, AlGhamdi J, Aldhafeeri FM, Embleton K, Morris D, Sluming V. 2011. Plasticity of the superior and middle cerebellar peduncles in musicians revealed by quantitative analysis of volume and number of streamlines based on diffusion tensor tractography. *Cerebellum* **10**:611–623. doi:10.1007/s12311-011-0274-1

Acer N, Bastepe-Gray S, Sagiroglu A, Gumus KZ, Degirmencioglu L, Zararsiz G, Ozic MU. 2018. Diffusion tensor and volumetric magnetic resonance imaging findings in the brains of professional musicians. *J Chem Neuroanat* **88**:33–40. doi:10.1016/j.jchemneu.2017.11.003

Andersson JLR, Sotiropoulos SN. 2016. An integrated approach to correction for off-resonance effects and subject movement in diffusion MR imaging. *NeuroImage* **125**:1063–1078. doi:10.1016/J.NEUROIMAGE.2015.10.019

Andoh J, Matsushita R, Zatorre RJ. 2015. Asymmetric Interhemispheric Transfer in the Auditory Network: Evidence from TMS, Resting-State fMRI, and Diffusion Imaging. *J Neurosci* **35**:14602–14611. doi:10.1523/JNEUROSCI.2333-15.2015

Annett M. 1970. A classification of hand preference by association analysis. *Br J Psychol* **61**:303–321. doi:10.1111/j.2044-8295.1970.tb01248.x

Ashburner J. 2007. A fast diffeomorphic image registration algorithm. *NeuroImage* **38**:95–113. doi:10.1016/J.NEUROIMAGE.2007.07.007

Athos EA, Levinson B, Kistler A, Zemansky J, Bostrom A, Freimer NB, Gitschier J. 2007. Dichotomy and perceptual distortions in absolute pitch ability. *Proc Natl Acad Sci U S A* **104**:14795–14800. doi:10.1073/pnas.0703868104

Basser PJ, Pierpaoli C. 2011. Microstructural and physiological features of tissues elucidated by quantitative-diffusion-tensor MRI. *J Magn Reson* **213**:560–570. doi:10.1016/J.JMR.2011.09.022

Behrens TEJ, Berg HJ, Jbabdi S, Rushworth MFS, Woolrich MW. 2007. Probabilistic diffusion tractography with multiple fibre orientations: What can we gain? *NeuroImage* **34**:144–155. doi:10.1016/J.NEUROIMAGE.2006.09.018

Behrens TEJ, Woolrich MW, Jenkinson M, Johansen-Berg H, Nunes RG, Clare S, Matthews PM, Brady JM, Smith SM. 2003. Characterization and propagation of uncertainty in diffusion-weighted MR imaging. *Magn Reson Med* **50**:1077–1088. doi:10.1002/mrm.10609

Behzadi Y, Restom K, Liau J, Liu TT. 2007. A component based noise correction method (CompCor) for BOLD and perfusion based fMRI. *NeuroImage* **37**:90–101. doi:10.1016/j.neuroimage.2007.04.042

Belden A, Zeng T, Przysinda E, Anteraper SA, Whitfield-Gabrieli S, Loui P. 2020. Improvising at rest: Differentiating jazz and classical music training with resting state functional connectivity. *NeuroImage* **207**:116384. doi:10.1016/j.neuroimage.2019.116384

Bengtsson SL, Nagy Z, Skare S, Forsman L, Forssberg H, Ullén F. 2005. Extensive piano practicing has regionally specific effects on white matter development. *Nat Neurosci* **8**:1148–1150. doi:10.1038/nn1516

Bermudez P, Zatorre RJ. 2009. A distribution of absolute pitch ability as revealed by computerized testing. *Music Percept Interdiscip J* **27**:89–101. doi:10.1525/mp.2009.27.2.89

Boekel W, Wagenmakers E-J, Belay L, Verhagen J, Brown S, Forstmann BU. 2015. A purely confirmatory replication study of structural brain-behavior correlations. *Cortex* **66**:115–133. doi:10.1016/J.CORTEX.2014.11.019

Bouhali F, Mongelli V, Thiebaut de Schotten M, Cohen L. 2020. Reading music and words: The anatomical connectivity of musicians' visual cortex. *NeuroImage* **212**:116666. doi:10.1016/j.neuroimage.2020.116666

Brauchli C, Leipold S, Jäncke L. 2020. Diminished large-scale functional brain networks in absolute pitch during the perception of naturalistic music and audiobooks. *NeuroImage* **216**:116513. doi:10.1016/j.neuroimage.2019.116513

Brauchli C, Leipold S, Jäncke L. 2019. Univariate and multivariate analyses of functional networks in absolute pitch. *NeuroImage* **189**:241–247. doi:10.1016/J.NEUROIMAGE.2019.01.021

Bressler SL, Menon V. 2010. Large-scale brain networks in cognition: emerging methods and principles. *Trends Cogn Sci* **14**:277–290. doi:10.1016/J.TICS.2010.04.004

Burkhard A, Hänggi J, Elmer S, Jäncke L. 2020. The importance of the fibre tracts connecting the planum temporale in absolute pitch possessors. *NeuroImage* **211**:116590. doi:10.1016/j.neuroimage.2020.116590

Button KS, Ioannidis JPA, Mokrysz C, Nosek BA, Flint J, Robinson ESJ, Munafò MR. 2013. Power failure: why small sample size undermines the reliability of neuroscience. *Nat Rev Neurosci* **14**:365–376. doi:10.1038/nrn3475

Chartrand J-P, Belin P. 2006. Superior voice timbre processing in musicians. *Neurosci Lett* **405**:164–167. doi:10.1016/j.neulet.2006.06.053

Damoiseaux JS, Greicius MD. 2009. Greater than the sum of its parts: a review of studies combining structural connectivity and resting-state functional connectivity. *Brain Struct Funct* **213**:525–533. doi:10.1007/s00429-009-0208-6

De Martino F, Valente G, Staeren N, Ashburner J, Goebel R, Formisano E. 2008. Combining multivariate voxel selection and support vector machines for mapping and classification of fMRI spatial patterns. *NeuroImage* **43**:44–58. doi:10.1016/j.neuroimage.2008.06.037

Deutsch D. 2013. Absolute pitchThe Psychology of Music. Elsevier. pp. 141–182. doi:10.1016/B978-0-12-381460-9.00005-5

Dohn A, Garza-Villarreal EA, Chakravarty MM, Hansen M, Lerch JP, Vuust P. 2015. Gray- and white-matter anatomy of absolute pitch possessors. *Cereb Cortex* **25**:1379–1388. doi:10.1093/cercor/bht334

Drakesmith M, Caeyenberghs K, Dutt A, Lewis G, David AS, Jones DK. 2015. Overcoming the effects of false positives and threshold bias in graph theoretical analyses of neuroimaging data. *NeuroImage* **118**:313–333. doi:10.1016/J.NEUROIMAGE.2015.05.011

Elmer S, Hänggi J, Jäncke L. 2016. Interhemispheric transcallosal connectivity between the left and right planum temporale predicts musicianship, performance in temporal speech processing, and functional specialization. *Brain Struct Funct* **221**. doi:10.1007/s00429-014-0910-x

Elmer S, Rogenmoser L, Kühnis J, Jäncke L. 2015. Bridging the gap between perceptual and cognitive perspectives on absolute pitch. *J Neurosci* **35**:366–371. doi:10.1523/jneurosci.3009-14.2015

Fauvel B, Groussard M, Chételat G, Fouquet M, Landeau B, Eustache F, Desgranges B, Platel H. 2014. Morphological brain plasticity induced by musical expertise is accompanied by modulation of functional connectivity at rest. *NeuroImage* **90**:179–188. doi:10.1016/J.NEUROIMAGE.2013.12.065

Friederici AD. 2011. The brain basis of language processing: From structure to function. *Physiol Rev* **91**:1357–1392. doi:10.1152/physrev.00006.2011

Fujioka T, Ross B, Kakigi R, Pantev C, Trainor LJ. 2006. One year of musical training affects development of auditory cortical-evoked fields in young children. *Brain* **129**:2593–2608. doi:10.1093/brain/awl247

Gordon EE. 1989. Advanced Measures of Music Audiation. GIA Publications.

Greber M, Rogenmoser L, Elmer S, Jäncke L. 2018. Electrophysiological correlates of absolute pitch in a passive auditory oddball paradigm: A direct replication attempt. *eNeuro* **5**:ENEURO.0333-18.2018. doi:10.1523/ENEURO.0333-18.2018

Greicius MD, Supekar K, Menon V, Dougherty RF. 2009. Resting-state functional connectivity reflects structural connectivity in the default mode network. *Cereb Cortex* **19**:72–78. doi:10.1093/cercor/bhn059

Griffiths TD, Warren JD. 2002. The planum temporale as a computational hub. *Trends Neurosci* **25**:348–353. doi:10.1016/S0166-2236(02)02191-4

Gujing L, Hui H, Xin L, Lirong Z, Yutong Y, Guofeng Y, Jing L, Shulin Z, Lei Y, Cheng L, Dezhong Y. 2019. Increased Insular Connectivity and Enhanced Empathic Ability Associated with Dance/Music Training. *Neural Plast* **2019**:9693109. doi:10.1155/2019/9693109

Habibi A, Damasio A, Ilari B, Veiga R, Joshi AA, Leahy RM, Haldar JP, Varadarajan D, Bhushan C, Damasio H. 2018. Childhood Music Training Induces Change in Micro and Macroscopic Brain Structure: Results from a Longitudinal Study. *Cereb Cortex* **28**:4336–4347. doi:10.1093/cercor/bhx286

Hallquist MN, Hillary FG. 2019. Graph theory approaches to functional network organization in brain disorders: A critique for a brave new small-world. *Netw Neurosci* **3**:1–26. doi:10.1162/netn_a_00054

Halwani GF, Loui P, Rüber T, Schlaug G. 2011. Effects of practice and experience on the arcuate fasciculus: Comparing singers, instrumentalists, and non-musicians. *Front Psychol* **2**:156–156. doi:10.3389/fpsyg.2011.00156

Haynes J-D. 2015. A primer on pattern-based approaches to fMRI: Principles, pitfalls, and perspectives. *Neuron* **87**:257–270. doi:10.1016/j.neuron.2015.05.025
Herholz SC, Zatorre RJ. 2012. Musical Training as a Framework for Brain Plasticity: Behavior, Function, and Structure. *Neuron* **76**:486–502. doi:10.1016/j.neuron.2012.10.011
Hermundstad AM, Bassett DS, Brown KS, Aminoff EM, Clewett D, Freeman S, Frithsen A, Johnson A, Tipper CM, Miller MB, Grafton ST, Carlson JM. 2013. Structural foundations of resting-state and task-based functional connectivity in the human brain. *Proc Natl Acad Sci* **110**:6169–6174. doi:10.1073/pnas.1219562110
Hickok G, Poeppel D. 2007. The cortical organization of speech processing. *Nat Rev Neurosci* **8**:393–402. doi:10.1038/nrn2113
Hofer S, Frahm J. 2006. Topography of the human corpus callosum revisited—Comprehensive fiber tractography using diffusion tensor magnetic resonance imaging. *NeuroImage* **32**:989–994. doi:10.1016/j.neuroimage.2006.05.044
Honey CJ, Sporns O, Cammoun L, Gigandet X, Thiran JP, Meuli R, Hagmann P. 2009. Predicting human resting-state functional connectivity from structural connectivity. *Proc Natl Acad Sci* **106**:2035–2040. doi:10.1073/pnas.0811168106
Hyde KL, Lerch J, Norton A, Forgeard M, Winner E, Evans AC, Schlaug G. 2009. Musical training shapes structural brain development. *J Neurosci* **29**:3019–3025. doi:10.1523/JNEUROSCI.5118-08.2009
Imfeld A, Oechslin MS, Meyer M, Loenneker T, Jäncke L. 2009. White matter plasticity in the corticospinal tract of musicians: A diffusion tensor imaging study. *NeuroImage* **46**:600–607. doi:10.1016/j.neuroimage.2009.02.025
Jäncke L. 2009. The plastic human brain. *Restor Neurol Neurosci* **27**:521–538. doi:10.3233/RNN-2009-0519
Jäncke L, Langer N, Hänggi J. 2012. Diminished whole-brain but enhanced peri-sylvian connectivity in absolute pitch musicians. *J Cogn Neurosci* **24**:1447–1461. doi:10.1162/jocn_a_00227
Jäncke L, Steinmetz H. 1998. Brain size: a possible source of interindividual variability in corpus callosum morphology In: E. Zaidel, M. Iacoboni, A. P. Pascual-Leone, editors. The Role of the Human Corpus Callosum in Sensory Motor Integration: Anatomy, Physiology, and Behavior; Individual Differences and Clinical Applications. New York, NY: Plenum Press.
Jäncke L, Steinmetz H. 1994. Interhemispheric transfer time and corpus callosum size. *NeuroReport* **5**:2385–2388.
Jeffreys H. 1961. Theory of probability, 3rd ed. Oxford University Press.
Kass RE, Raftery AE. 1995. Bayes factors. *J Am Stat Assoc* **90**:773–795. doi:10.1080/01621459.1995.10476572
Kim S-G, Knösche TR. 2017. Resting state functional connectivity of the ventral auditory pathway in musicians with absolute pitch. *Hum Brain Mapp* **38**:3899–3916. doi:10.1002/hbm.23637
Kim S-G, Knösche TR. 2016. Intracortical myelination in musicians with absolute pitch: Quantitative morphometry using 7-T MRI. *Hum Brain Mapp* **37**:3486–3501. doi:10.1002/hbm.23254
Klein C, Liem F, Hänggi J, Elmer S, Jäncke L. 2016. The “silent” imprint of musical training. *Hum Brain Mapp* **37**:536–546. doi:10.1002/hbm.23045
Kraus N, Chandrasekaran B. 2010. Music training for the development of auditory skills. *Nat Rev Neurosci* **11**:599–605. doi:10.1038/nrn2882
Langer N, Pedroni A, Jäncke L. 2013. The problem of thresholding in small-world network analysis. *PLoS ONE* **8**:e53199–e53199. doi:10.1371/journal.pone.0053199
Leipold S, Brauchli C, Greber M, Jäncke L. 2019a. Absolute and relative pitch processing in the human brain: neural and behavioral evidence. *Brain Struct Funct* **224**:1723–1738. doi:10.1007/s00429-019-01872-2
Leipold S, Greber M, Sele S, Jäncke L. 2019b. Neural patterns reveal single-trial information on absolute pitch and relative pitch perception. *NeuroImage* **200**:132–141. doi:10.1016/J.NEUROIMAGE.2019.06.030
Leipold S, Oderbolz C, Greber M, Jäncke L. 2019c. A reevaluation of the electrophysiological correlates of absolute pitch and relative pitch: No evidence for an absolute pitch-specific negativity. *Int J Psychophysiol* **137**:21–31. doi:10.1016/j.ijpsycho.2018.12.016
Loui P, Li HC, Hohmann A, Schlaug G. 2011. Enhanced cortical connectivity in absolute pitch musicians: a model for local hyperconnectivity. *J Cogn Neurosci* **23**:1015–1026. doi:10.1162/jocn.2010.21500
Loui P, Zamm A, Schlaug G. 2012. Enhanced functional networks in absolute pitch. *NeuroImage* **63**:632–640. doi:10.1016/j.neuroimage.2012.07.030

Luo C, Guo Z, Lai Y, Liao W, Liu Q, Kendrick KM, Yao D, Li H. 2012. Musical Training Induces Functional Plasticity in Perceptual and Motor Networks: Insights from Resting-State fMRI. *PLoS ONE* **7**:e36568–e36568. doi:10.1371/journal.pone.0036568

Luo C, Tu S, Peng Y, Gao S, Li J, Dong L, Li G, Lai Y, Li H, Yao D. 2014. Long-term effects of musical training and functional plasticity in salience system. *Neural Plast* **2014**. doi:10.1155/2014/180138

Magne C, Schön D, Besson M. 2006. Musician Children Detect Pitch Violations in Both Music and Language Better than Nonmusician Children: Behavioral and Electrophysiological Approaches. *J Cogn Neurosci* **18**:199–211. doi:10.1162/jocn.2006.18.2.199

Maris E, Oostenveld R. 2007. Nonparametric statistical testing of EEG- and MEG-data. *J Neurosci Methods* **164**:177–190. doi:10.1016/j.jneumeth.2007.03.024

McKetton L, DeSimone K, Schneider KA. 2019. Larger auditory cortical area and broader frequency tuning underlie absolute pitch. *J Neurosci* 1532–18. doi:10.1523/JNEUROSCI.1532-18.2019

Mesulam M-M. 1990. Large-scale neurocognitive networks and distributed processing for attention, language, and memory. *Ann Neurol* **28**:597–613. doi:10.1002/ana.410280502

Münte TF, Altenmüller E, Jäncke L. 2002. The musician's brain as a model of neuroplasticity. *Nat Rev Neurosci* **3**:473–478. doi:10.1038/nrn843

Nichols TE, Holmes AP. 2002. Nonparametric permutation tests for functional neuroimaging: A primer with examples. *Hum Brain Mapp* **15**:1–25. doi:10.1002/hbm.1058

Oechslin MS, Imfeld A, Loenneker T, Meyer M, Jäncke L. 2010a. The plasticity of the superior longitudinal fasciculus as a function of musical expertise: A diffusion tensor imaging study. *Front Hum Neurosci* **3**. doi:10.3389/neuro.09.076.2009

Oechslin MS, Meyer M, Jäncke L. 2010b. Absolute pitch — functional evidence of speech-relevant auditory acuity. *Cereb Cortex* **20**:447–455. doi:10.1093/cercor/bhp113

Öztürk AH, Tasçioglu B, Aktekin M, Kurtoglu Z, Erden I. 2002. Morphometric comparison of the human corpus callosum in professional musicians and non- musicians by using in vivo magnetic resonance imaging. *J Neuroradiol* **29**:29–34.

Palomar-García MÁ, Zatorre RJ, Ventura-Campos N, Bueichekú E, Ávila C. 2017. Modulation of Functional Connectivity in Auditory-Motor Networks in Musicians Compared with Nonmusicians. *Cereb Cortex* **27**:2768–2778. doi:10.1093/cercor/bhw120

Pantev C, Oostenveld R, Engelien A, Ross B, Roberts LE, Hoke M. 1998. Increased auditory cortical representation in musicians. *Nature* **392**:811–814.

Penhune VB. 2011. Sensitive periods in human development: Evidence from musical training. *Cortex* **47**:1126–1137. doi:10.1016/j.cortex.2011.05.010

Power JD, Barnes KA, Snyder AZ, Schlaggar BL, Petersen SE. 2012. Spurious but systematic correlations in functional connectivity MRI networks arise from subject motion. *NeuroImage* **59**:2142–2154. doi:10.1016/J.NEUROIMAGE.2011.10.018

Power JD, Fair DA, Schlaggar BL, Petersen SE. 2010. The Development of Human Functional Brain Networks. *Neuron* **67**:735–748. doi:10.1016/j.neuron.2010.08.017

Power JD, Plitt M, Laumann TO, Martin A. 2017. Sources and implications of whole-brain fMRI signals in humans. *NeuroImage* **146**:609–625. doi:10.1016/J.NEUROIMAGE.2016.09.038

Rauschecker JP, Scott SK. 2009. Maps and streams in the auditory cortex: nonhuman primates illuminate human speech processing. *Nat Neurosci* **12**:718–724. doi:10.1038/nn.2331

Roland JL, Snyder AZ, Hacker CD, Mitra A, Shimony JS, Limbrick DD, Raichle ME, Smyth MD, Leuthardt EC. 2017. On the role of the corpus callosum in interhemispheric functional connectivity in humans. *Proc Natl Acad Sci* **114**:13278–13283. doi:10.1073/pnas.1707050114

Rouder JN, Morey RD, Speckman PL, Province JM. 2012. Default Bayes factors for ANOVA designs. *J Math Psychol* **56**:356–374. doi:10.1016/J.JMP.2012.08.001

Rouder JN, Speckman PL, Sun D, Morey RD, Iverson G. 2009. Bayesian t tests for accepting and rejecting the null hypothesis. *Psychon Bull Rev* **16**:225–237. doi:10.3758/PBR.16.2.225

Rüber T, Lindenberg R, Schlaug G. 2015. Differential Adaptation of Descending Motor Tracts in Musicians. *Cereb Cortex* **25**:1490–1498. doi:10.1093/cercor/bht331

Rubinov M, Sporns O. 2010. Complex network measures of brain connectivity: Uses and interpretations. *NeuroImage* **52**:1059–1069. doi:10.1016/j.neuroimage.2009.10.003

Schlaug G. 2015. Musicians and music making as a model for the study of brain plasticity In: Altenmüller E, Finger S, Boller F, editors. Progress in Brain Research, Music, Neurology, and Neuroscience: Evolution, the Musical Brain, Medical Conditions, and Therapies. Elsevier. pp. 37–55. doi:10.1016/bs.pbr.2014.11.020

Schlaug G, Forgeard M, Zhu L, Norton Andrea, Norton Andrew, Winner E. 2009. Training-induced neuroplasticity in young children. *Ann N Y Acad Sci* **1169**:205–208. doi:10.1111/j.1749-6632.2009.04842.x

Schlaug G, Jäncke L, Huang Y, Staiger JF, Steinmetz H. 1995. Increased corpus callosum size in musicians. *Neuropsychologia* **33**:1047–1055. doi:10.1016/0028-3932(95)00045-5

Schmithorst VJ, Wilke M. 2002. Differences in white matter architecture between musicians and non-musicians: A diffusion tensor imaging study. *Neurosci Lett* **321**:57–60. doi:10.1016/S0304-3940(02)00054-X

Schneider P, Scherg M, Dosch HG, Specht HJ, Gutschalk A, Rupp A. 2002. Morphology of Heschl's gyrus reflects enhanced activation in the auditory cortex of musicians. *Nat Neurosci* **5**:688–694. doi:10.1038/nn871

Schulze K, Mueller K, Koelsch S. 2013. Auditory stroop and absolute pitch: an fMRI study. *Hum Brain Mapp* **34**:1579–1590. doi:10.1002/hbm.22010

Seither-Preisler A, Parncutt R, Schneider P. 2014. Size and Synchronization of Auditory Cortex Promotes Musical, Literacy, and Attentional Skills in Children. *J Neurosci* **34**:10937–10949. doi:10.1523/JNEUROSCI.5315-13.2014

Smith SM, Jenkinson M, Woolrich MW, Beckmann CF, Behrens TEJ, Johansen-Berg H, Bannister PR, De Luca M, Drobnjak I, Flitney DE, Niazy RK, Saunders J, Vickers J, Zhang Y, De Stefano N, Brady JM, Matthews PM. 2004. Advances in functional and structural MR image analysis and implementation as FSL. *NeuroImage* **23, Supple**:S208–S219. doi:10.1016/j.neuroimage.2004.07.051

Smith SM, Nichols TE. 2009. Threshold-free cluster enhancement: Addressing problems of smoothing, threshold dependence and localisation in cluster inference. *NeuroImage* **44**:83–98. doi:10.1016/j.neuroimage.2008.03.061

Sporns O, Chialvo DR, Kaiser M, Hilgetag CC. 2004. Organization, development and function of complex brain networks. *Trends Cogn Sci* **8**:418–425. doi:10.1016/J.TICS.2004.07.008

Steele CJ, Bailey JA, Zatorre RJ, Penhune VB. 2013. Early musical training and white-matter plasticity in the corpus callosum: Evidence for a sensitive period. *J Neurosci* **33**:1282–1290. doi:10.1523/JNEUROSCI.3578-12.2013

Uddin LQ, Supekar K, Lynch CJ, Khouzam A, Phillips J, Feinstein C, Ryali S, Menon V. 2013. Salience Network–Based Classification and Prediction of Symptom Severity in Children With Autism. *JAMA Psychiatry* **70**:869–869. doi:10.1001/jamapsychiatry.2013.104

van den Heuvel MP, de Lange SC, Zalesky A, Seguin C, Yeo BTT, Schmidt R. 2017. Proportional thresholding in resting-state fMRI functional connectivity networks and consequences for patient-control connectome studies: Issues and recommendations. *NeuroImage* **152**:437–449. doi:10.1016/j.neuroimage.2017.02.005

van der Knaap LJ, van der Ham IJM. 2011. How does the corpus callosum mediate interhemispheric transfer? A review. *Behav Brain Res* **223**:211–221. doi:10.1016/j.bbr.2011.04.018

Van Wijk BCM, Stam CJ, Daffertshofer A. 2010. Comparing brain networks of different size and connectivity density using graph theory. *PLoS ONE* **5**. doi:10.1371/journal.pone.0013701

Vollmann H, Ragert P, Conde V, Villringer A, Classen J, Witte OW, Steele CJ. 2014. Instrument specific use-dependent plasticity shapes the anatomical properties of the corpus callosum: a comparison between musicians and non-musicians. *Front Behav Neurosci* **8**:245. doi:10.3389/fnbeh.2014.00245

Wengenroth M, Blatow M, Heinecke A, Reinhardt J, Stippich C, Hofmann E, Schneider P. 2014. Increased volume and function of right auditory cortex as a marker for absolute pitch. *Cereb Cortex* **24**:1127–1137. doi:10.1093/cercor/bhs391

Wenhart T, Bethlehem RAI, Baron-Cohen S, Altenmüller E. 2019. Autistic traits, resting-state connectivity, and absolute pitch in professional musicians: shared and distinct neural features. *Mol Autism* **10**:20–20. doi:10.1186/s13229-019-0272-6

Winkler AM, Ridgway GR, Webster MA, Smith SM, Nichols TE. 2014. Permutation inference for the general linear model. *NeuroImage* **92**:381–397. doi:10.1016/J.NEUROIMAGE.2014.01.060

Witelson SF. 1989. Hand and sex differences in the isthmus and genu of the human corpus callosum: a postmortem morphological study. *Brain* **112**:799–835. doi:10.1093/brain/112.3.799

Wong PCM, Skoe E, Russo NM, Dees T, Kraus N. 2007. Musical experience shapes human brainstem encoding of linguistic pitch patterns. *Nat Neurosci* **10**:420–422. doi:10.1038/nn1872

Xia M, Wang J, He Y. 2013. BrainNet Viewer: A network visualization tool for human brain connectomics. *PLoS ONE* **8**:e68910–e68910. doi:10.1371/journal.pone.0068910

Yan C-G, Wang X-D, Zuo X-N, Zang Y-F. 2016. DPABI: Data Processing & Analysis for (Resting-State) Brain Imaging. *Neuroinformatics* **14**:339–351. doi:10.1007/s12021-016-9299-4

Yan C-G, Zang Y. 2010. DPARSF: a MATLAB toolbox for “pipeline” data analysis of resting-state fMRI. *Front Syst Neurosci* **4**:13–13. doi:10.3389/fnsys.2010.00013

Yendiki A, Koldewyn K, Kakunoori S, Kanwisher N, Fischl B. 2014. Spurious group differences due to head motion in a diffusion MRI study. *NeuroImage* **88**:79–90. doi:10.1016/J.NEUROIMAGE.2013.11.027

Zalesky A, Fornito A, Bullmore ET. 2010. Network-based statistic: Identifying differences in brain networks. *NeuroImage* **53**:1197–1207. doi:10.1016/j.neuroimage.2010.06.041

Zamorano AM, Cifre I, Montoya P, Riquelme I, Kleber B. 2017. Insula-based networks in professional musicians: Evidence for increased functional connectivity during resting state fMRI. *Hum Brain Mapp* **38**:4834–4849. doi:10.1002/hbm.23682

Zamorano AM, Montoya P, Cifre I, Vuust P, Riquelme I, Kleber B. 2019. Experience-dependent neuroplasticity in trained musicians modulates the effects of chronic pain on insula-based networks – A resting-state fMRI study. *NeuroImage* **202**:116103. doi:10.1016/j.neuroimage.2019.116103

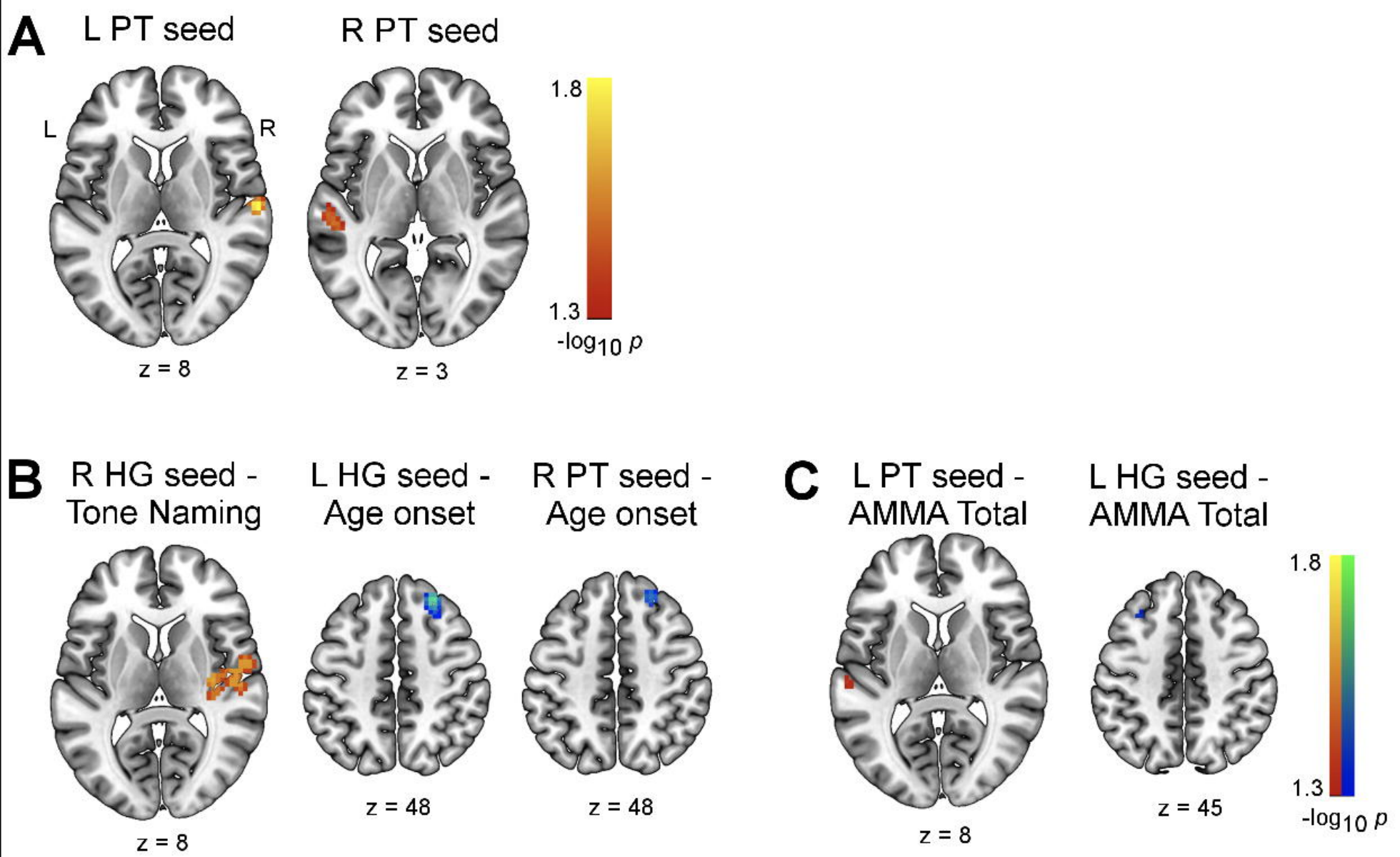
A
L PT seed
R PT seed
L
R
z = 8
z = 3
1.8
1.3
-log10 p
B
R HG seed - Tone Naming
L HG seed - Age onset
R PT seed - Age onset
z = 8
z = 48
z = 48
C
L PT seed - AMMA Total
L HG seed - AMMA Total
z = 8
z = 45
1.8
1.3
-log10 p

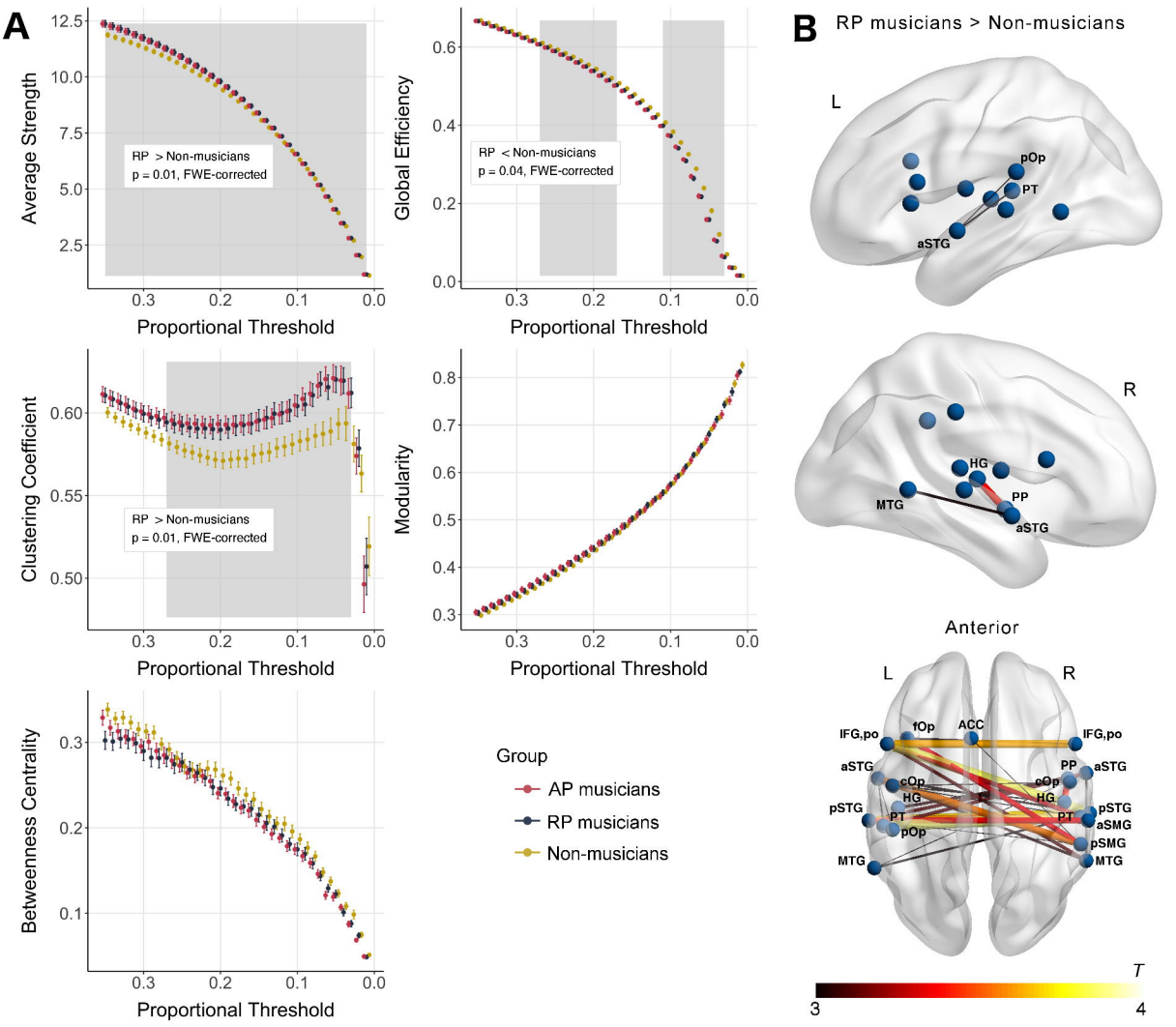
A
Average Strength
RP > Non-musicians
p = 0.01, FWE-corrected
Proportional Threshold
Global Efficiency
RP < Non-musicians
p = 0.04, FWE-corrected
Proportional Threshold
Clustering Coefficient
RP > Non-musicians
p = 0.01, FWE-corrected
Proportional Threshold
Modularity
Proportional Threshold
Betweenness Centrality
Proportional Threshold
Group
AP musicians
RP musicians
Non-musicians
B
RP musicians > Non-musicians
L
pOp
PT
aSTG
R
HG
PP
MTG
aSTG
Anterior
L
R
lFG,po
fOp
ACC
lFG,po
aSTG
cOp
HG
pSTG
PT
pOp
MTG
PP
aSTG
pOp
HG
pSTG
PT
aSMG
pSMG
MTG
T
3
4

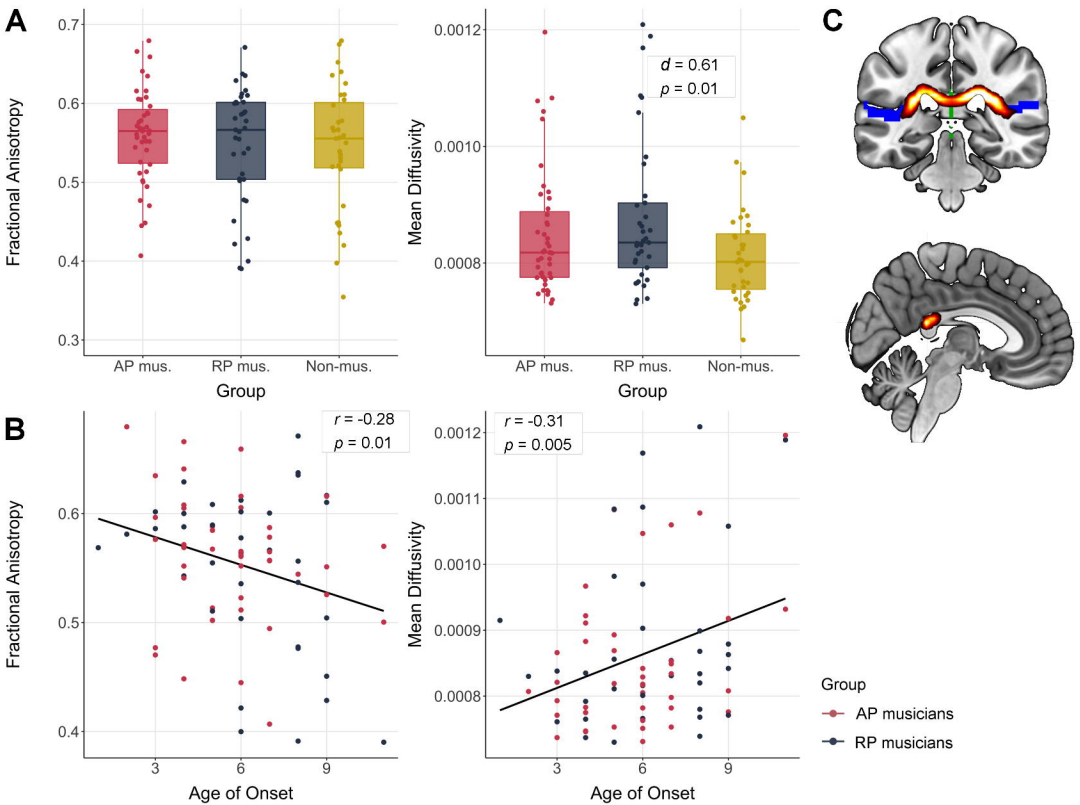
A
Fractional Anisotropy
0.7
0.6
0.5
0.4
0.3
AP mus.
RP mus.
Non-mus.
Group
Mean Diffusivity
0.0012
0.0010
0.0008
d = 0.61
p = 0.01
AP mus.
RP mus.
Non-mus.
Group
C
B
Fractional Anisotropy
0.6
0.5
0.4
r = -0.28
p = 0.01
3
6
9
Age of Onset
Mean Diffusivity
0.0012
0.0011
0.0010
0.0009
0.0008
r = -0.31
p = 0.005
3
6
9
Age of Onset
Group
AP musicians
RP musicians

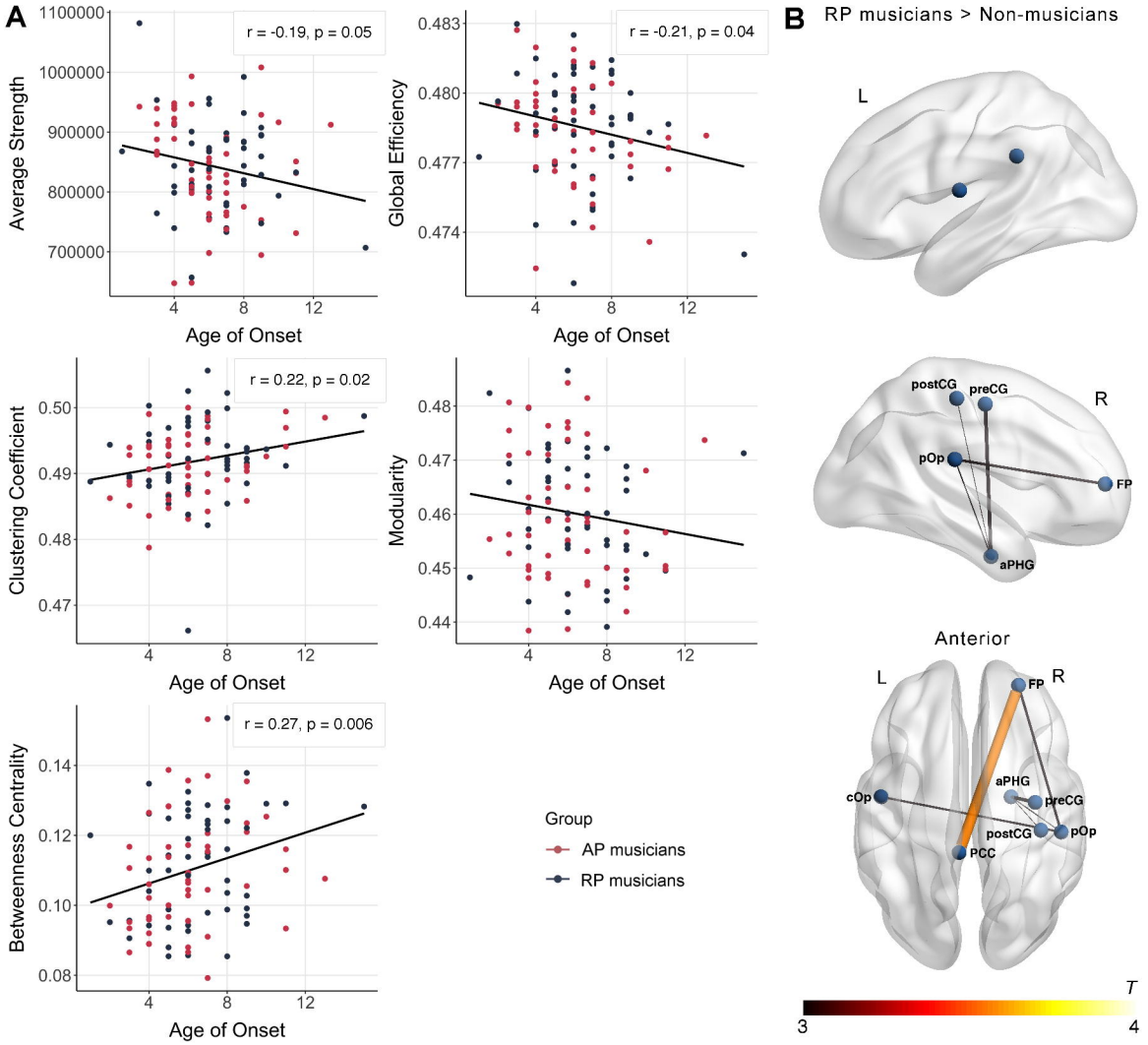
A
r = -0.19, p = 0.05
Average Strength
Age of Onset
r = -0.21, p = 0.04
Global Efficiency
Age of Onset
r = 0.22, p = 0.02
Clustering Coefficient
Age of Onset
Modularity
Age of Onset
r = 0.27, p = 0.006
Betweenness Centrality
Age of Onset
Group
AP musicians
RP musicians
B
RP musicians > Non-musicians
L
R
postCG
preCG
pOp
FP
aPHG
Anterior
L
R
FP
aPHG
preCG
cOp
postCG
pOp
PCC
T
3
4